A STUDY OF LONG–TERM STABILITY OF ATOMIC CLOCKS

David W. Allan
National Bureau of Standards
Time and Frequency Division
325 Broadway
Boulder, Colorado 80303

ABSTRACT

The importance of long–term frequency stability has increased significantly in recent years because of the discovery of the millisecond pulsar, PSR 1937+21. In addition, long–term stability is extremely useful not only in evaluating primary frequency standards and the performance of national timing centers, but also in addressing questions regarding autonomy for the Global Positioning System (GPS) and syntonization for Jet Propulsion Laboratory's (JPL) Deep Space Tracking Network.

Over the last year, NBS has carried out several studies addressing questions regarding the long–term frequency stability of different kinds of atomic clocks as well as of principal timing centers. These analyses cover commercial and primary cesium–beam frequency standards; active hydrogen maser frequency standards and the new commercial mercury–ion frequency standards at United States Naval Observatory (USNO).

The support and cooperation of the timing centers involved have, along with the GPS common–view measurement technique, made these analyses possible. Fortunately, the measurement noise was significantly less than the clock noise for the long–term stability regions studied. Fractional frequency stabilities, $\sigma_y(\tau)$, of parts in 10^{14} down to parts in 10^{15} were observed for various of these standards. It is believed that frequency stabilities on the order of a part in 10^{15} will be necessary to measure the effects of gravity waves on frequency stability between millisecond pulsars and atomic clocks on or near the earth.

INTRODUCTION

The primary reasons for improved long–term stability in atomic clocks have been the study of millisecond pulsars[1,2], autonomy questions for GPS, maintaining syntonization for the JPL Deep Space Network and long term stability performance of new clocks at the primary timing centers throughout the world. As needs have arisen for improved stability in atomic time scales, several laboratories have responded with very strong efforts in producing new standards[3–8]. Some analysis techniques to ascertain current performance of the best operating clocks in the world have also been developed. Fortunately, the GPS common–view time–difference and frequency–difference measurement technique has allowed us to analyze long–term clock time deviations at state–of–the–art levels.

One analysis tool used was a statistical cross–correlation technique in the time domain in order to ascertain correlations at different integration times[1]. This tool was developed to study long term correlations in the presence of nonstationary processes in the clock deviations. The next tool was to employ the NBS algorithm for generating the time scale NBS(AT1) from the ensemble of clocks at NBS[9]. NBS(AT1) plus an equation generates UTC(NBS); the latter being the official time from the National Bureau of Standards. This same algorithm was used on the international set of clocks available through GPS common–view measurements. Each laboratory timing center's output was treated as an

Report Documentation Page

Public reporting burden for the collection of information is estimated to average 1 hour per response, including the time for reviewing instructions, searching existing data sources, gathering and maintaining the data needed, and completing and reviewing the collection of information. Send comments regarding this burden estimate or any other aspect of this collection of information, including suggestions for reducing this burden, to Washington Headquarters Services, Directorate for Information Operations and Reports, 1215 Jefferson Davis Highway, Suite 1204, Arlington VA 22202-4302. Respondents should be aware that notwithstanding any other provision of law, no person shall be subject to a penalty for failing to comply with a collection of information if it does not display a currently valid OMB control number.

1. REPORT DATE	2. REPORT TYPE	3. DATES COVERED
DEC 1987		**00-00-1987 to 00-00-1987**

4. TITLE AND SUBTITLE	5a. CONTRACT NUMBER
A Study of Long-Term Stability of Atomic Clocks	5b. GRANT NUMBER
	5c. PROGRAM ELEMENT NUMBER

6. AUTHOR(S)	5d. PROJECT NUMBER
	5e. TASK NUMBER
	5f. WORK UNIT NUMBER

7. PERFORMING ORGANIZATION NAME(S) AND ADDRESS(ES)	8. PERFORMING ORGANIZATION REPORT NUMBER
National Bureau of Standards,Time and Frequency Division,325 Broadway,Boulder,CO,80303	

9. SPONSORING/MONITORING AGENCY NAME(S) AND ADDRESS(ES)	10. SPONSOR/MONITOR'S ACRONYM(S)
	11. SPONSOR/MONITOR'S REPORT NUMBER(S)

12. DISTRIBUTION/AVAILABILITY STATEMENT
Approved for public release; distribution unlimited

13. SUPPLEMENTARY NOTES
Proceedings of the Nineteenth Annual Precise Time and Time Interval (PTTI) Applications and Planning Meeting, Redondo Beach, CA, 1-3 Dec 1987

14. ABSTRACT
see report

15. SUBJECT TERMS

16. SECURITY CLASSIFICATION OF:			17. LIMITATION OF ABSTRACT	18. NUMBER OF PAGES	19a. NAME OF RESPONSIBLE PERSON
a. REPORT	b. ABSTRACT	c. THIS PAGE	**Same as Report (SAR)**	**38**	
unclassified	**unclassified**	**unclassified**			

independent clock and then combined with all the others in an optimum minimum squared error sense according to the NBS algorithm's design. The hope is to generate a "world's best" clock, which in turn could be used to analyze each of the constituent members and then better understand the long term stability performance of each. The next tool used was an N–cornered hat statistical approach under the assumption of independence of the member clocks[10]. In this way we can sort out the performance of each member of a set of N clocks in terms of its statistical characteristics. Last, a second–difference drift estimator was used to study long term frequency drift correlations among some of the clocks involved[10,11].

Figure 1 shows a plot of the fractional frequency stability between the millisecond pulsar (PSR 1937+21) and UTC(NBS), as well as the stability estimate of NBS(AT1) versus the "world's best" clock estimate. Figure 1 shows that with more integration time the millisecond pulsar might show better performance than the best clocks in the world. As indicated in the plot the possibility of measuring gravity waves at a few parts in 10^{15} at integration times of the order of a year is by itself a significant motivator.

GENERATION OF THE "WORLD'S BEST" CLOCK AND COMPARISON OF THE PERFORMANCE OF THE INTERNATIONAL TIMING CENTERS

The advantage of post–analysis is that we can more easily discern outliers and abnormal performance in the member clocks. Following this post analysis and removal of outliers and abnormal behavior, we can then employ optimal statistical processing techniques. These processing techniques can approach the ideal once the nonstochastic behavior has been filtered off. In contrast, the time from any timing center, including the generation of TAI has to be calculated or generated in near real time. In a real–time operation, subtle frequency steps and annual variations cannot readily be dealt with because of their low frequency character. Often they are best observed in post–analysis.

A period of time commensurate with the installation of the new measurement system for the millisecond pulsar (PSR1937+21) at Arecibo, Puerto Rico was picked. The time was a 1110 day period from MJD 45769 to MJD 46879. The data not available on the NBS computer file were accrued from the Princeton University computer file or were extracted from the BIH annual report. The UTC scales were used from the various timing centers as they were more readily available. Since some of the UTC scales are steered, we tried to remove the steering corrections so that the contributing scales would be independent. The post–analysis was performed removing known frequency steps in the time scales and outliers that would contaminate the stochastic analysis.

An N–cornered hat analysis between the times generated by the various timing centers was first performed in order to get a first order estimate of the 10 day stability and the longer term stability of each of the outputs from the timing centers. Preliminary parameters were then chosen for the optimization routine for the NBS algorithm to include each timing center's output as a clock member. One of the features of the NBS algorithm is that it is an adaptive filter so that as a clock improves or degrades with time the filtered estimate will adapt to the value commensurate with the clock's performance. The time constant of this filter for this experiment was set at three months. Once the parameters have been set and the clocks processed through the NBS algorithm, the "world's best" estimate could then be used to better ascertain the performance of each member clock, and the parameters could be appropriately fine tuned to reduce the minimum squared error of the estimate of the ensemble as well as of each individual member. Figures 2a and 2b through 14a and 14b list a modified $\sigma_y(\tau)$ fractional frequency stability plot and a time residual plot with a mean frequency and a mean time removed for each of the contributing timing centers. The abscissas and ordinates have been kept the same in the figures for convenience of comparison.

The contributing timing centers were: Applied Physics Laboratory at Johns Hopkins University, Laurel, MD; Commonwealth Scientific and Industrial Research Organization, Australia; Istituto Elettrotecnico Nazionale, Torino, Italy; National Bureau of Standards, Boulder, CO; National Physical Laboratory, Teddington, England; National Research Council in Ottawa, Canada; Paris Observatory, Paris, France; Physikalisch–Technische Bundesantalt, Braunschweig, Germany; Radio Research Laboratory Tokyo, Japan; and Tokyo Astronomical Observatory, Tokyo, Japan; Technische Universität Gras, Gras, Austria; US Naval Observatory, Washington, DC; and Van Swinden Laboratory, Delft, Netherlands.

Following are some highlights to note from the several figures. Though there was a limited set of data available on the hydrogen maser at APL, the stability at integration times of a few months is very impressive. The NBS algorithm generates from its own ensemble a scale called AT1, which is neither synchronized nor syntonized with any other scale. NBS(AT1) is optimized for frequency stability. Because NBS(AT1) had the largest weight among the set of clocks used in this "world's best" estimate, we removed it from the ensemble and looked at it independently against all the other optimally weighted clocks in order to see whether a similar stability performance was still obtained. This independent analysis confirmed the stability plots shown in Figures 5a and 5b.

Most of the timing centers have clock output stabilities at levels of a few parts in 10^{14} for integration times from 10 days out to the order of a year. Figures 9a and 9b for PTB show exceedingly good stability from year to year, though there may be inadequate confidence of the estimate to confirm this. This stability may be because UTC(PTB) is steered with their primary cesium clock. Also annual variations appear in the time deviations of the PTB output. The excellent performance of the TUG clock may be because this single commercial clock is temperature controlled, humidity controlled and voltage controlled. The apparent quadratic behavior observed in the residuals of the USNO clock is of concern because most of these clocks are high performance cesium beam clocks. We are led to ask whether there is a systematic frequency drift in a particular production line series. On the other hand, the month–to–month stability is very good.

A STUDY OF THE ANNUAL VARIATIONS

For the most stringent of timing users, B. Guinot at the International Bureau of Weights and Measures (BIPM) has generated a scale called Terrestrial Time BIPM TT(BIPM). Figure 15 shows the fractional frequency differences between TT(BIPM) and International Atomic Time (TAI) over the last several years. The noticeable frequency step is associated with the 1972 adjustment in the SI second used for TAI to conform with the NBS, NRC and PTB primary frequency standards. Annual variations are apparent between these two scales. Since PTB Cs 1 is believed to be one of the best primary clocks in the world, its weight in generating TT(BIPM) is quite high, and the annual term shown earlier in the PTB plot in Figures 9a and 9b corresponds with the annual variations shown in Figure 15. We are led to the questions: are these annual variations in all of the clocks in the world ensemble, moving up and down together on an annual basis, or are they in PTB Cs 1, or a combination of both? At the few parts in 10^{14} level it is very difficult to ascertain which conclusion is the most nearly correct.

In an effort to obtain an independent estimate regarding this problem, the data from the millisecond pulsar were analyzed. The pulsar data have much larger variations from week to week and month to month — primarily due to the 4 k parsec (13,000 light–years) path of the signal. The variations can be fairly well characterized as a white noise phase modulation (PM) process at about the 300 ns level. Because such noise integrates as $\tau^{-3/2}$ on a mod $\sigma_y(\tau)$ plot, the long term variations can be meaningful. PSR1937+21 is plotted against PTB Cs 1 in Figure 16. Also plotted in Figure 16 are the time difference residuals between PTB Cs 1 and NBS(AT1). Visually, correlations are apparent even though masked

somewhat by the pulsar data noise.

To further study the significance of these annual variations we incorporated a cross–correlation analysis tool[1]. The correlations seemed statistically significant for integration times longer than several months. From this study, the annual variations seem to be primarily in PTB Cs 1; however, this is inconclusive because in the generation of the pulsar data, an annual term had to be removed in conjunction with the determination of the ephemeris for the earth as it orbits the sun. Further study is needed before a definite conclusion can be obtained.

STUDY OF THE COMMERCIAL MERCURY ION STANDARD'S FREQUENCY STABILITIES

Three independent clocks were chosen to study the stability of the two commercial mercury–ion standards located at USNO [6]. Data on the unit called No. 2 covered about a 1 year period and the data on No. 3 covered the last one–half year period. As can be seen in the fractional frequency stability plots shown in Figures 17a, 18a and 19a, there are missing data and some abnormal behavior during the first several weeks of the data. This first part was segmented off for the statistical analysis period, which was from 19 December 1986 to 14 November 1987. The stabilities plotted in Figures 17b, 18b and 19b are for the segmented period.

Assuming independence, the four clocks (unsteered UTC(USNO), NBS(AT1), the APL hydrogen maser and the mercury ion No. 2) were compared in an N–cornered hat analysis. That data are plotted in Figure 20.

For integration times of one, two and four days the GPS common–view noise contaminated the data for APL and NBS. It appears that the NBS and USNO outputs have a flicker frequency modulation (FM) like performance at about a part in 10^{14} over this 11 month data set. The long term frequency drift in the APL hydrogen maser is apparent. The excellent stability performance of the mercury ion standard — as the winner in this 4–cornered hat analysis for integration times of a week to a month — is also apparent. The one, two and four day stability values plotted may be pessimistic, as they are contaminated with measurement noise. However, there appears to be some stability degeneration for integration times of the order of a few months and longer. For completeness the other pair–wise members of the 4–cornered hat are shown in Figures 21a and b through 23a and b.

Over the last one–half year we studied the stability difference between the two commercial mercury–ion standards No. 2 and No. 3. Figures 24a and b show a most outstanding performance of these two standards. Since the stability plotted in Figure 24 is inconsistent with that plotted in Figure 20, we asked whether No. 1 and No. 2 were correlated. To study whether these two clocks have long term correlations and to be able to define a cross–correlation coefficient as a function of τ called $\rho(\tau)$ we proceeded as follows[10]. Given fractional frequency differences:

$$y_1 = \text{clock i} - \text{clock j and}$$

$$y_2 = \text{clock k} - \text{clock l,}$$

we can compute a variance of the difference

$$\sigma^2_{y_1 - y_2}(\tau) = \sigma^2_{y_1}(\tau) - 2\sigma_{y_1 y_2}(\tau) + \sigma^2_{y_2}(\tau)$$

We construct:

$$\rho(\tau) = \frac{\sigma_{y_1 y_2}(\tau)}{\sigma_{y_1}(\tau) \cdot \sigma_{y_2}(\tau)}.$$

378

At a given τ, if $\rho(\tau)$ approached +1 then we could conclude that there are correlations between i and k, or j and l, or -i and l, or -k and j. If $\rho(\tau)$ approached -1, then we could conclude that there are correlations between -i and k, or -j and l, or i and l, or k and j. This cross-correlation analysis was tested with simulated data and gave affirmative results to the above conclusions and to the ability to test in the presence of low frequency divergence processes such as flicker noise FM and random walk FM. Figure 25 would indicate that some of the long–term instabilities are in fact due to mercury–ion No. 2. Figure 26a and b would indicate that No. 2 and No. 3 are positively correlated for integration times of a few months. Using different references, Figures 27a and b lead us to the same conclusion as similarly do Figures 28a and b. All three independent clock pairs lead to the same conclusion that mercury–ion standards No. 2 and No. 3 appear to be long term correlated for integration times of a few months. Figure 29a would indicate no statistical correlation between the four clocks involved. On the other hand Figure 29b shows a definite positive cross–correlation; this is believed to be due to the fact that over the half year analyzed mercury–ion standard No. 2 and the APL maser had positive frequency drifts.

The following independent test of the hypotheses that the low frequency variations could be modelled by long–term correlations between the two mercury ion standards and frequency drifts between the APL maser and the mercury ion standards, was conducted. Frequency drifts were measured using a second difference estimator over the last half year with respect to NBS(AT1) UTC(USNO–unsteered) and the UTC(PTB) time scales. UTC(PTB) has as its reference the PTB primary Cs 1 standard. We observe a very high correlation in the frequency drift numbers measured with respect to the different laboratories (Figure 30). Within this small sample of three clocks, the drifts seem to be statistically significant — indicating, again, that in long term the two mercury ion standards appear to be correlated, and that the frequency drifts of the APL hydrogen maser and the ion standards are in the same direction.

The correlation mechanism is not yet understood and is being studied. Environmental perturbations due to temperature, temperature gradients and pressure are possible candidates. The very outstanding performance of these mercury ion standards gives great hope that if this problem can be identified and fixed, these standards will have a major contribution in the long–term stability analysis of the best frequency standards known.

CONCLUSIONS

The long term frequency stability of time scales has improved dramatically over the last few years. This study has revealed that additional long term frequency stability improvements may be possible if the cause of annual variations in clocks can be identified and fixed. Also, if frequency drift problems can be solved, and if cross–correlation problems through the environment can be identified and fixed, the next few years should show significant improvements in the performance of hydrogen masers and of mercury–ion frequency standards.

It is also apparent from this study that algorithms for combining clock readings can significantly impact the performance of a computed time scale. The NBS algorithm implemented seemed to have merit even where there were significant differences in statistical characteristics of the member clocks contributing to the ensemble.

who helped process a large amount of the data.

REFERENCES

[1] D.W. Allan, Millisecond Pulsar Rivals Best Atomic Clock Stability, Proceedings of the 41st Annual Symposium on Frequency Control, May 27–29 1987, pp. 2–11.

[2] L.A. Rawley, J.H. Taylor, M.M. Davis, and D.W. Allan, Millisecond Pulsar PSR 1937+21: A Highly Stable Clock, Science 238, 761–764 (1987).

[3] D.J. Wineland, Trapped Ions, Laser Cooling, and Better Clocks, Science, 226, 395–400, (1984).

[4] A. DeMarchi, New Insights into Causes and Cures of Frequency Instabilities (Drift and Long Term Noise) in Cesium, Proceedings of the 41st Annual Symposium on Frequency Control, May 27–29, 1987, pp. 53–58.

[5] J.C. Bergquist, W.M. Itano, and D.J. Wineland, Recoilless Optical Absorption and Doppler Sidebands in a Single Trapped Ion, Phys. Rev. A, 36, 428 (1987).

[6] L.S. Cutler, R.P. Giffard, P.J. Wheeler, and G.M.R. Winkler, Initial Operational Experience with a Mercury Ion Storage Frequency Standard, Proceedings of the 41st Annual Symposium on Frequency Control, May 27–29, 1987 pp. 12–19.

[7] F.L. Walls, Characteristics and Performance of Miniature NBS Passive Hydrogen Masers, IEEE Trans. Instr. and Meas., IM–36, 596–603 (1987).

[8] H. Peters, B. Owings, and T. Oakley, Sigma Tau Standards Corporation and L. Beno, Proceedings of the 41st Annual Symposium on Frequency Control, May 27–29, 1987, pp. 75–81.

[9] F.B. Varnum, D.R. Brown, D.W. Allan, and T.K. Peppler, Comparison of Time Scales Generated with the NBS Ensembling Algorithm, 19th Annual Precise Time and Time Interval Applications and Planning Meeting, Dec. 1, 1987

[10] D. W. Allan. Time and Frequency (Time–Domain) Characterization, Estimation, and Prediction of Precision Clocks and Oscillators, IEEE 1987 New Trans. on UFFC.

[11] J.A. Barnes, The Measurement of Linear Frequency Drift in Oscillators, Proceedings of 15th Annual Precise Time and Time Interval Meeting, December 1983, pp. 551–579.

Figure Captions

Figure 1. The open hexagons are a plot of the fractional frequency stability (square root of the modified Allan variance) mod.$\sigma_y(\tau)$ versus τ for the millisecond pulsar as compared against UTC(NBS). The solid hexagons are a plot of an estimate of the stability of the NBS(AT1) time scale as compared against a world's "best clock". Also indicated is where one might measure gravity wave radiation effects between the earth and the millisecond pulsar.

Figures 2a and b through 14a and b. Fractional frequency stability (square root of the Allan variance) $\sigma_y(\tau)$ vs. τ and the time residual plot for the various timing centers as estimated against a world's "best clock" ensemble calculated by using the NBS algorithm.

Figure 15. A plot of the frequency difference between a special terrestrial time scale generated by the International Bureau of Weights and Measures TT(BIPM) and International Atomic Time (TAI). Annual variations are evident. The noticeable frequency change at 1 January 1972 was in TAI, and was purposefully inserted to bring the second of TAI into agreement with the SI second as given by the primary frequency standards.

Figure 16. A plot of the time–difference residuals between PTB Cs 1 and the millisecond pulsar, PSR 1937+21, and the heavy line is a plot of the time– difference residuals between PTB Cs 1 and NBS(AT1). Some correlation is apparent.

Figures 17a and b through 19a and b are fractional frequency stability plots of the commercial mercury–ion standard No. 2 against the three indicated independent reference standards.

Figure 20. A 4–cornered hat analysis estimate of the fractional frequency stability, $\sigma_y(\tau)$, of each of the following four independent time outputs: APL hydrogen maser, NBS(AT1), USNO(MC with steering corrections removed) and the commercial mercury–ion standard No. 2.

Figures 21a and b through 23a and b are fractional frequency stability plots of the other possible combinations of standards individually estimated in Figure 20 and not plotted in Figures 17a and b through 19a and b.

Figures 24a and b. Plots of the fractional frequency stability between two commercial mercury–ion standards, No. 2 and No. 3. The stabilities plotted beyond 10^6 seconds are among the best ever reported, but because of apparent correlations between these two standards the values in this range are probably too optimistic.

Figure 25. A plot of a cross correlation coefficient as a function of averaging time for 11 months data span. That the coefficient is near 1 for averaging times longer than about two months would indicate that the long–term deviations in the two sets of data cross–correlated are primarily due to the mercury–ion standard No. 2.

Figures 26a and b through 28a and b are cross–correlation plots as a function of averaging time to test if there are correlations between the two mercury–ion standards for the last half–year. The two mercury–ion standards were interchanged in their position in the cross–correlation analysis between the "a" figures and the "b" figures. All six of these figures are consistent with the hypothesis that there are significant positive correlations between the two mercury–ion standards for averaging times of the order of two months and some longer.

Figures 29a and b. Figure "a" would indicate that there is no significant correlation between the mercury–ion standard No. 2 and NBS(AT1) or between the APL H–maser and unsteered UTC(USNO). The positive correlation shown in Figure "b" can be explained by the apparent long–term negative frequency drift in both the APL H–maser and the mercury–ion standard No. 2; though logically, we cannot exclude the possibility of correlations between NBS(AT1) and unsteered UTC(USNO), which seems very unlikely.

Figure 30. A tabular listing of frequency drift estimates over the last half–year of data with respect to three principle timing centers with independent standards. This table shows a high degree of correlation between the two mercury–ion standards, and it also shows that the positive correlation shown in Figure 29b is likely due to the negative frequency drift in mercury–ion standard No. 2 and the APL H–maser.

⬡ ≡ MILLISECOND PULSAR PSR 1937+21 — UTC(NBS)
OCT.'84 — FEB.'87
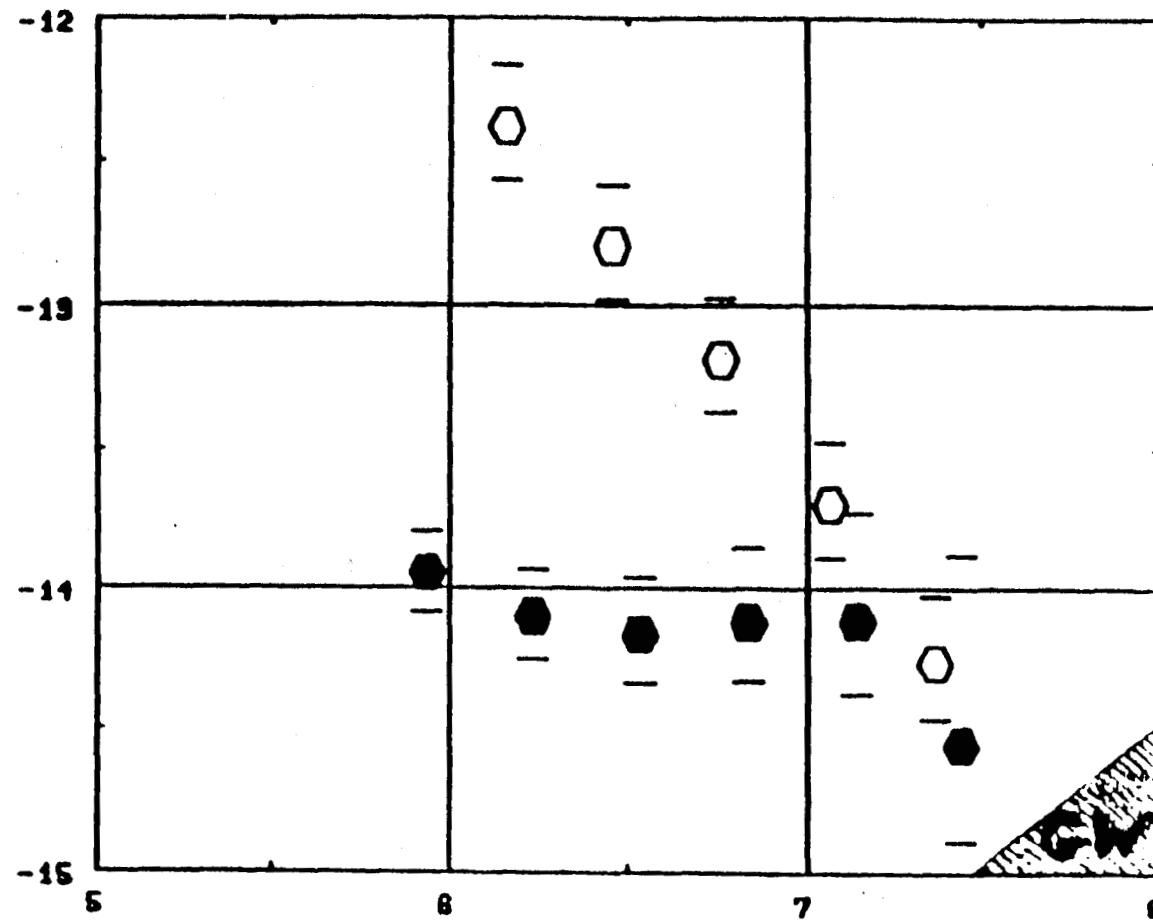
Figure 1

LOG TAU (Seconds)
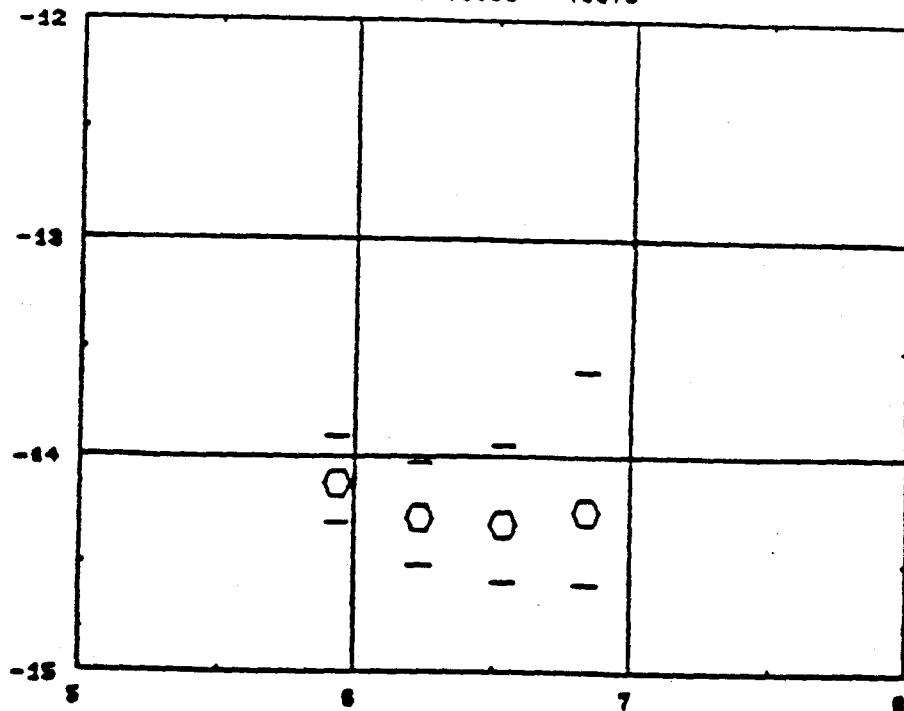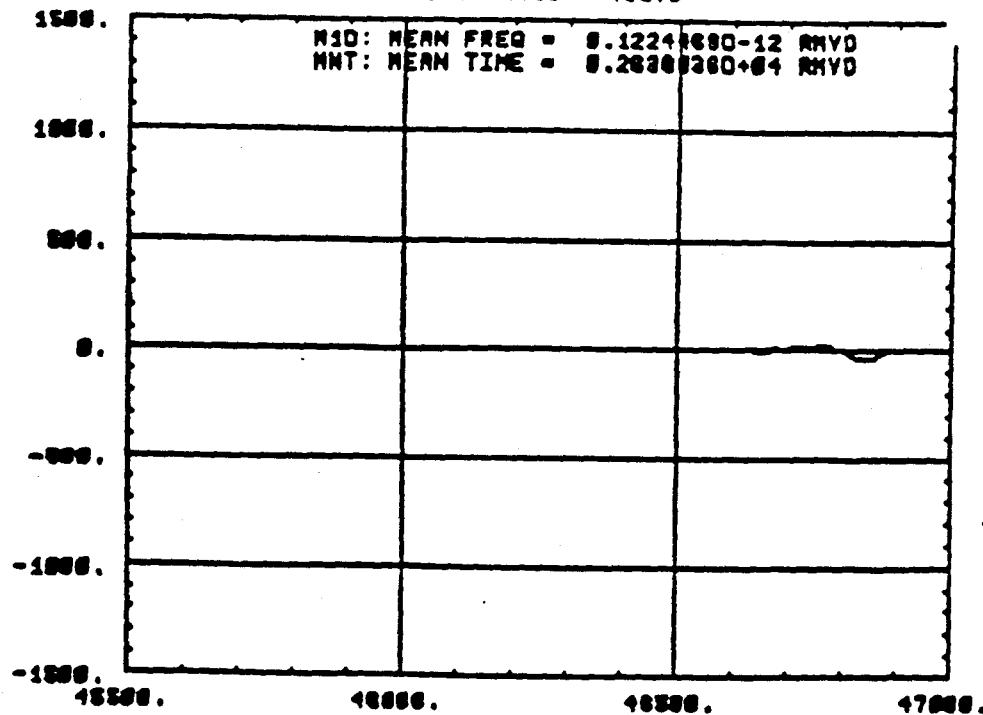
Figure 2a

Figure 2b

LOG MOD SIGy(TAU)

**CSIRO BEST ESTIMATE VIA NBS ALG.
MJD'S 46589 - 46879**
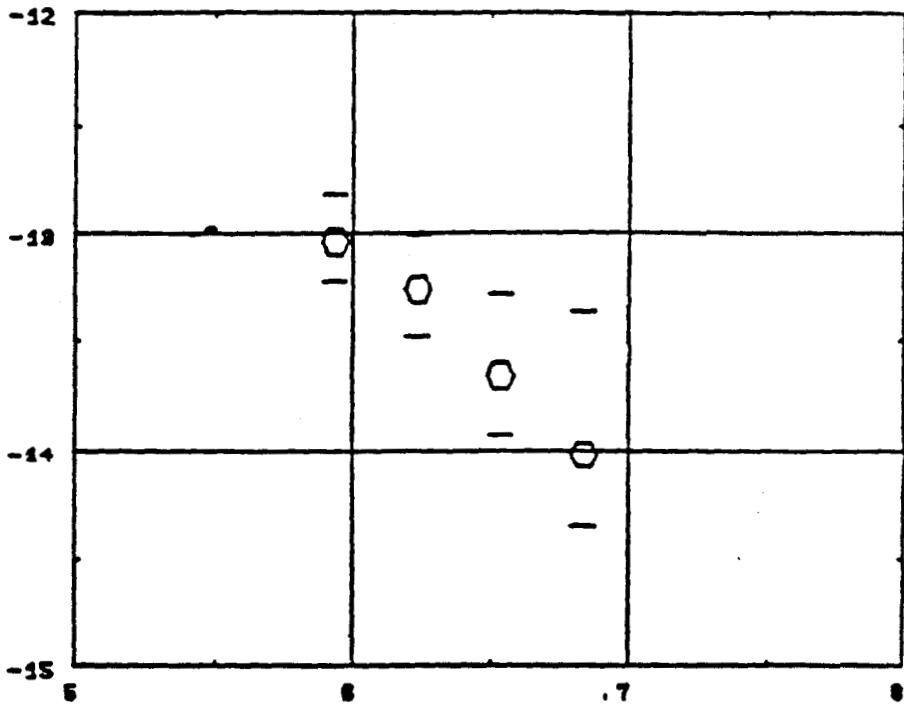
Figure 3a   LOG TAU (Seconds)

TIME (ns)

**CSIRO BEST ESTIMATE VIA NBS ALG.
MJD'S 46589 - 46879**

MJD: MEAN FREQ = 8.2846835D-12 RMVD
MNT: MEAN TIME = 8.5489480D+84 RMVD

Figure 3b   DAY (MJD)
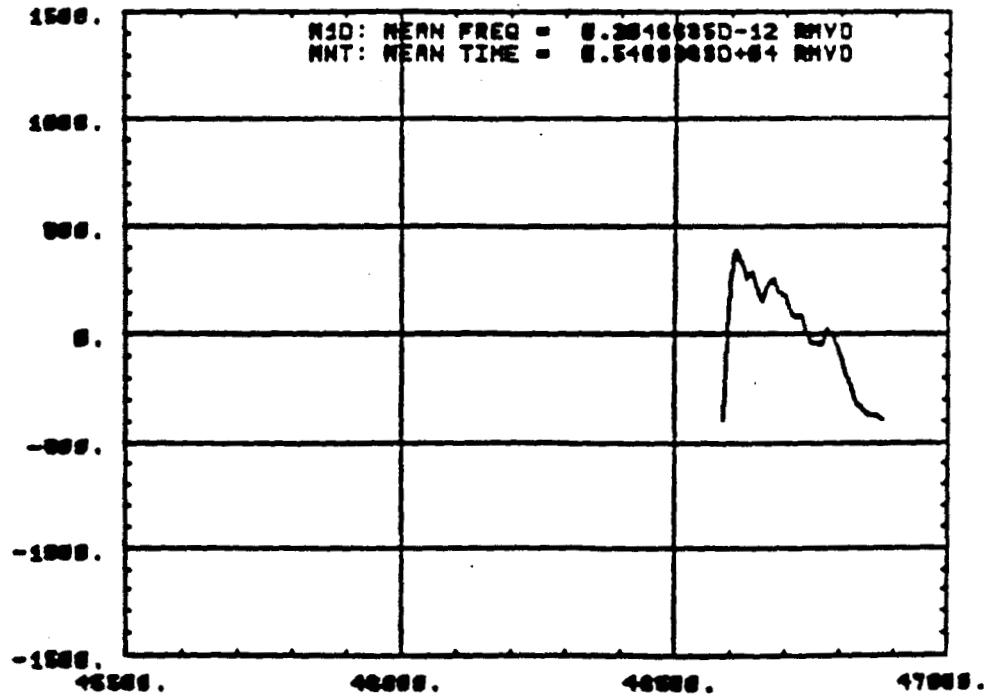
LOG MOD SIGy(TAU)

IEN BEST ESTIMATE VIA MBS ALG.
MJD'S 46578 - 46879

Figure 4a   LOG TAU (Seconds)

TIME (ns)

IEN BEST ESTIMATE VIA MBS ALG.
MJD'S 46578 - 46879
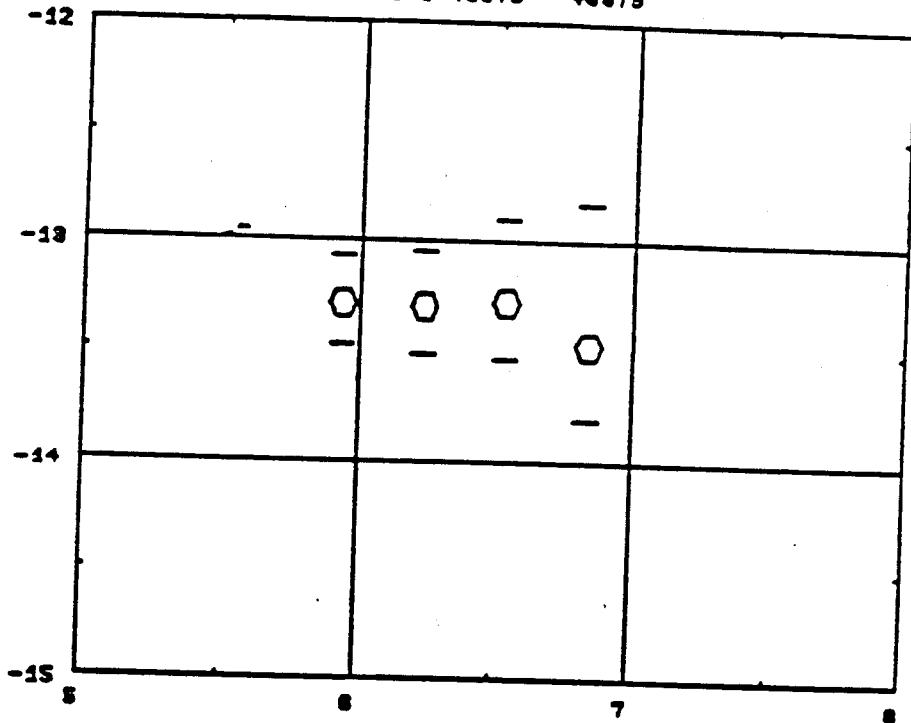
MID: MEAN FREQ = -0.16120380-12 RMVO
ANT: MEAN TIME = 0.2771710D+04 RMVO
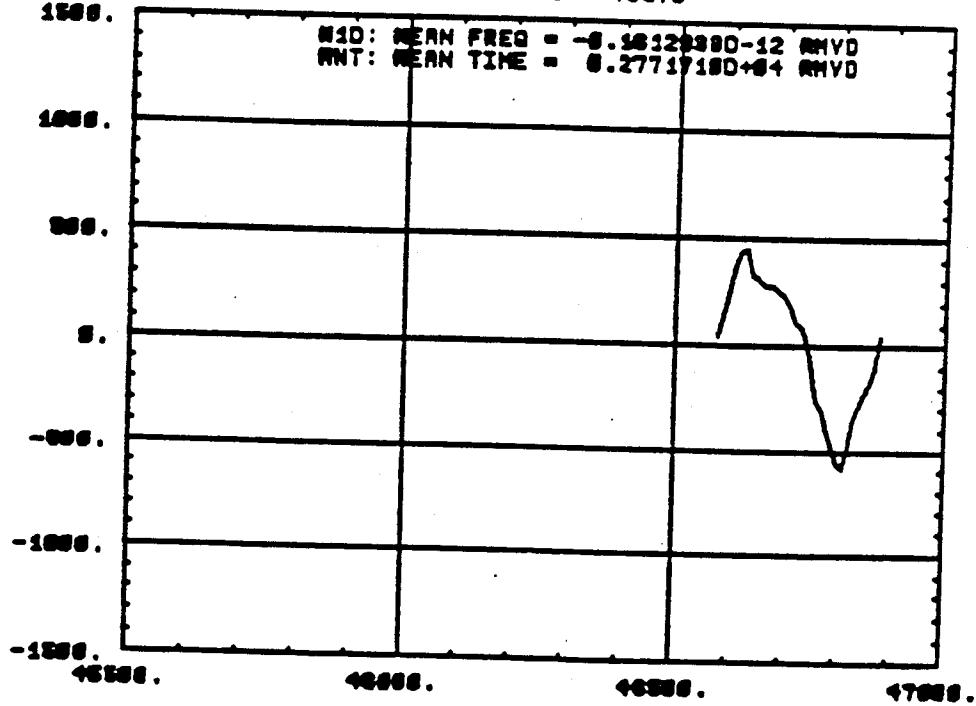
Figure 4b   DAY (MJD)

NBS(AT1) BEST ESTIMATE VIA NBS ALG.
MJD's 45769 - 46879

LOG MOD SISy(TAU)
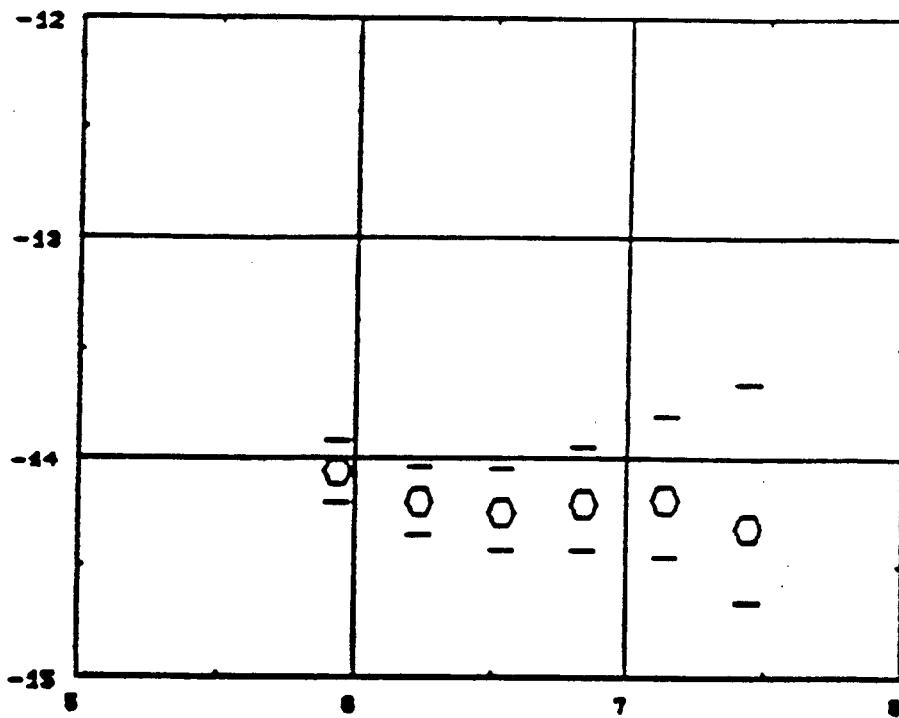
Figure 5a

LOG TAU (Seconds)

NBS(AT1) BEST ESTIMATE VIA NBS ALG.
MJD's 45769 - 46879

TIME (ns)

M1D: MEAN FREQ = 9.9865912D-13 PH"D
MMT: MEAN TIME = -9.1889730+03 RMVD

Figure 5b

DAY (MJD)

NPL BEST ESTIMATE VIA NBS ALG.
MJD'S 46589 - 46879

LOG MOD SIGy(TAU)

Figure 6a   LOG TAU (Seconds)

NPL BEST ESTIMATE VIA NBS ALG.
MJD'S 46589 - 46879

TIME (ns)

M1D: MEAN FREQ = -8.4827888D-14 RMYD
MNT: MEAN TIME = 8.4228158D+63 RMYD
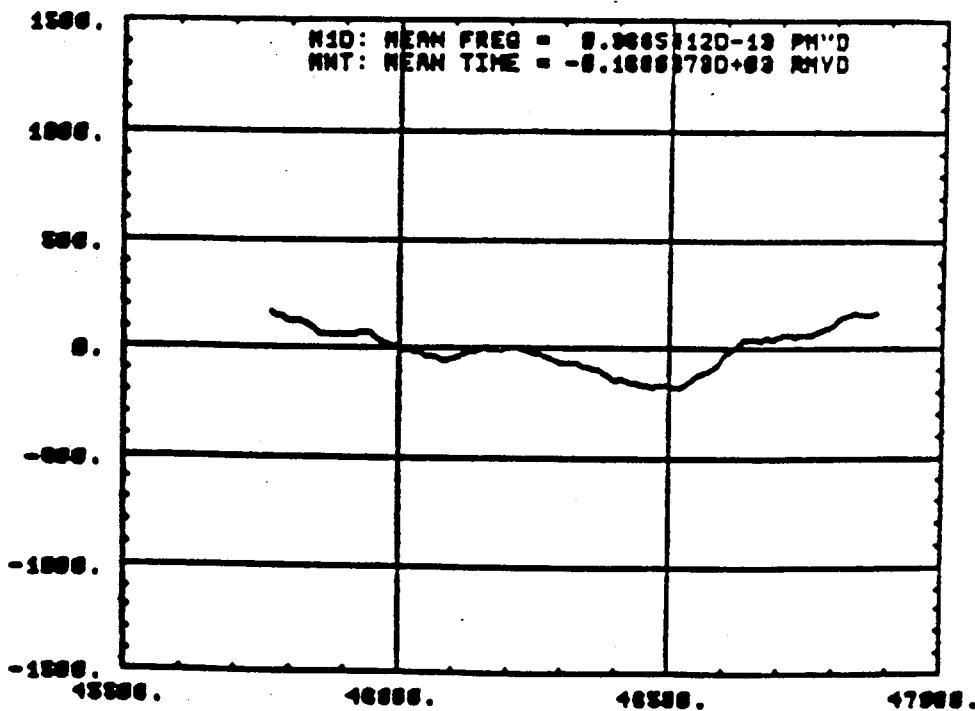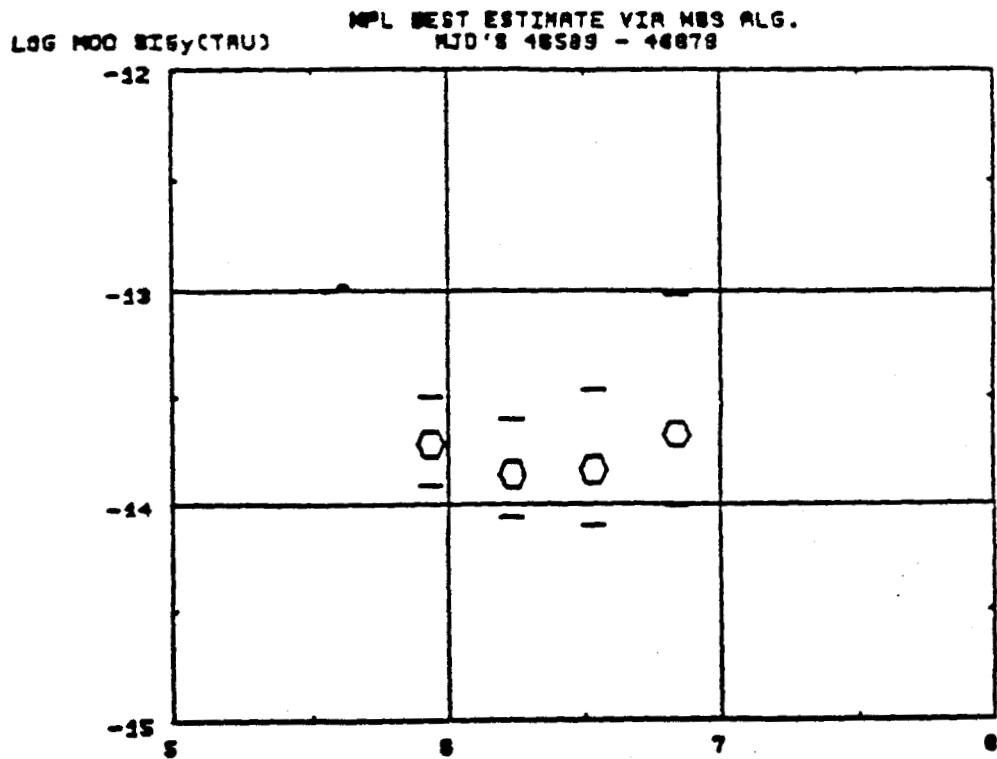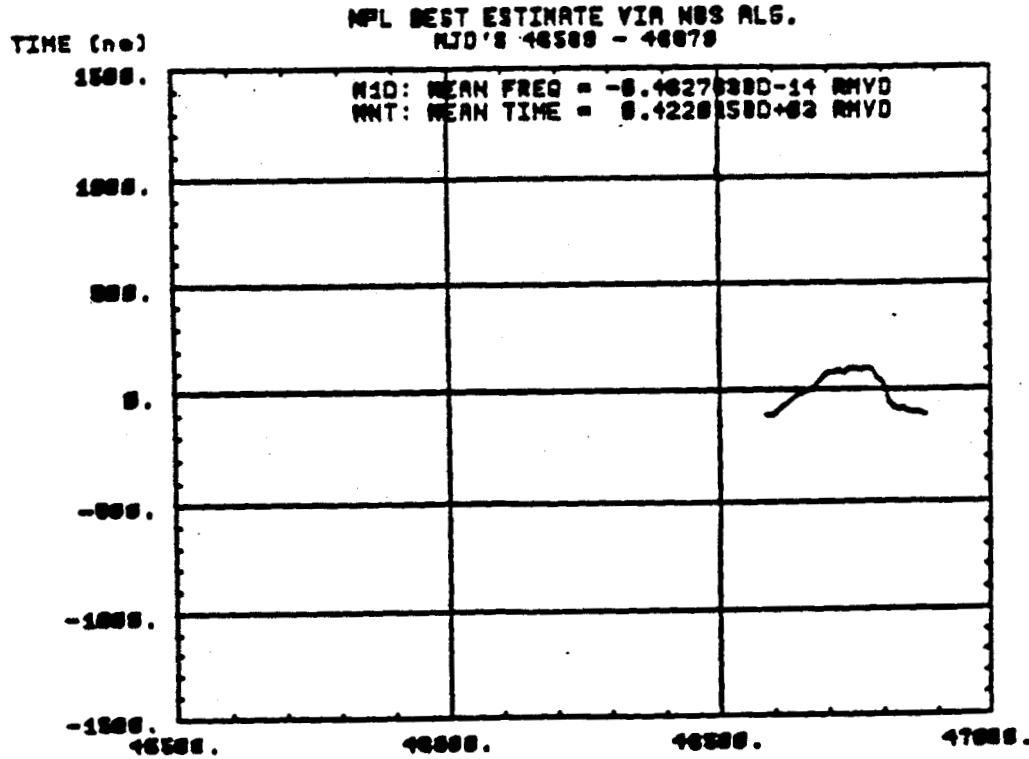
Figure 6b   DAY (MJD)

NRC Cs V BEST ESTIMATE VIA NBS ALG.
MJD'S 45899 - 46879

LOG MOD SIGy(TAU)
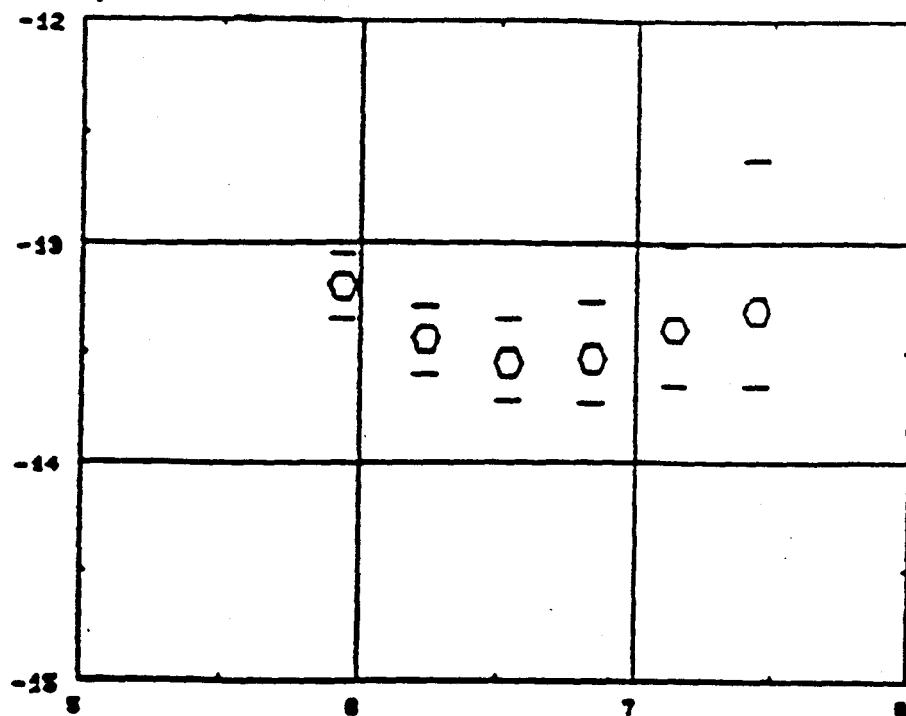
Figure 7a   LOG TAU (Seconds)

NRC Cs V BEST ESTIMATE VIA NBS ALG.
MJD 's 45899 - 46879

TIME (ns)

Figure 7b   DAY (MJD)

Figure 8a

Figure 8b

PTB Ca 1 BEST ESTIMATE VIA NBS ALG.
MJD'S 45769 - 46879

LOG MOD SIGy(TAU)

Figure 9a

LOG TAU (Seconds)

PTB Ca 1 BEST ESTIMATE VIA NBS ALG.
MJD'S 45769 - 46879

TIME (ns)

Figure 9b

DAY (MJD)

LOG MOD SIGy(TAU)

ARL BEST ESTIMATE VIA NBS ALG.
MJO'S 46129 - 46879

Figure 10a

LOG TAU (Seconds)

TIME (ns)

ARL BEST ESTIMATE VIA NBS ALG.
MJO'S 46129 - 46879

Figure 10b

DAY (MJO)

380-12

TAC BEST ESTIMATE VIA NBS ALG.
MJD'S 45858 - 46878

LOG MOD SISy(TAU)

Figure 11a   LOG TAU (Seconds)

TAC BEST ESTIMATE VIA NBS ALG.
MJD'S 45858 - 46878

TIME (ns)

Figure 11b   DAY (MJD)

Figure 12a

LOG TAU (Seconds)

Figure 13a   LOG TAU (Seconds)

Figure 13b   DAY (MJD)
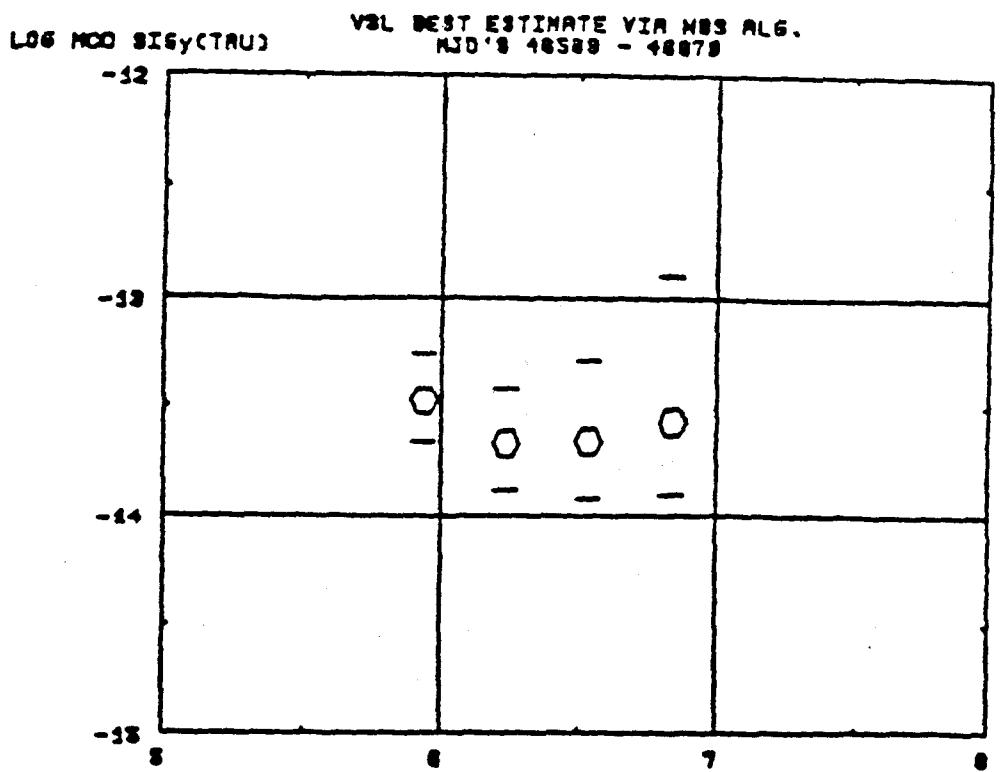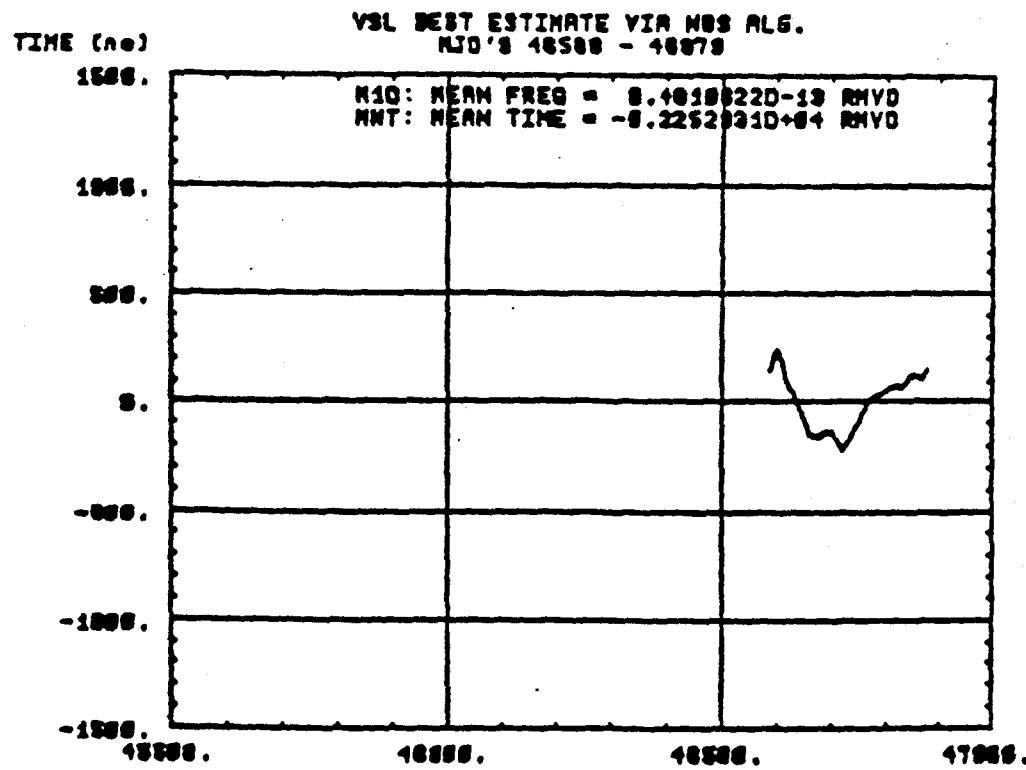
Figure 14a

Figure 14b

Figure 15

Figure 16

TIME (ns)

DAY (MJD)

380-18

Figure 17a

DAT (MJD)

LOG SIGMAy(TAU)

Hg ION #2 - APL H-MASER
13 DEC.'86 - 14 NOV.'87
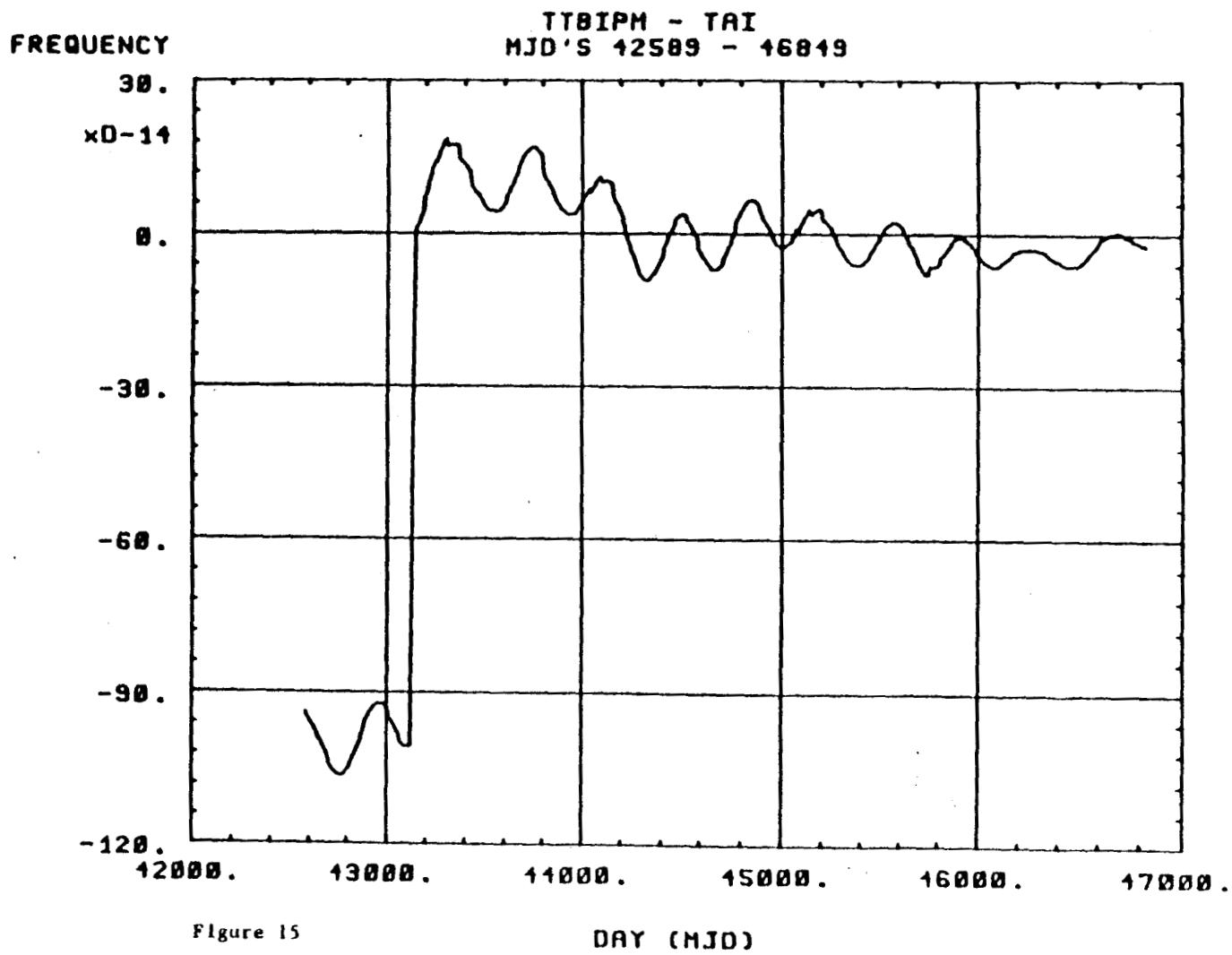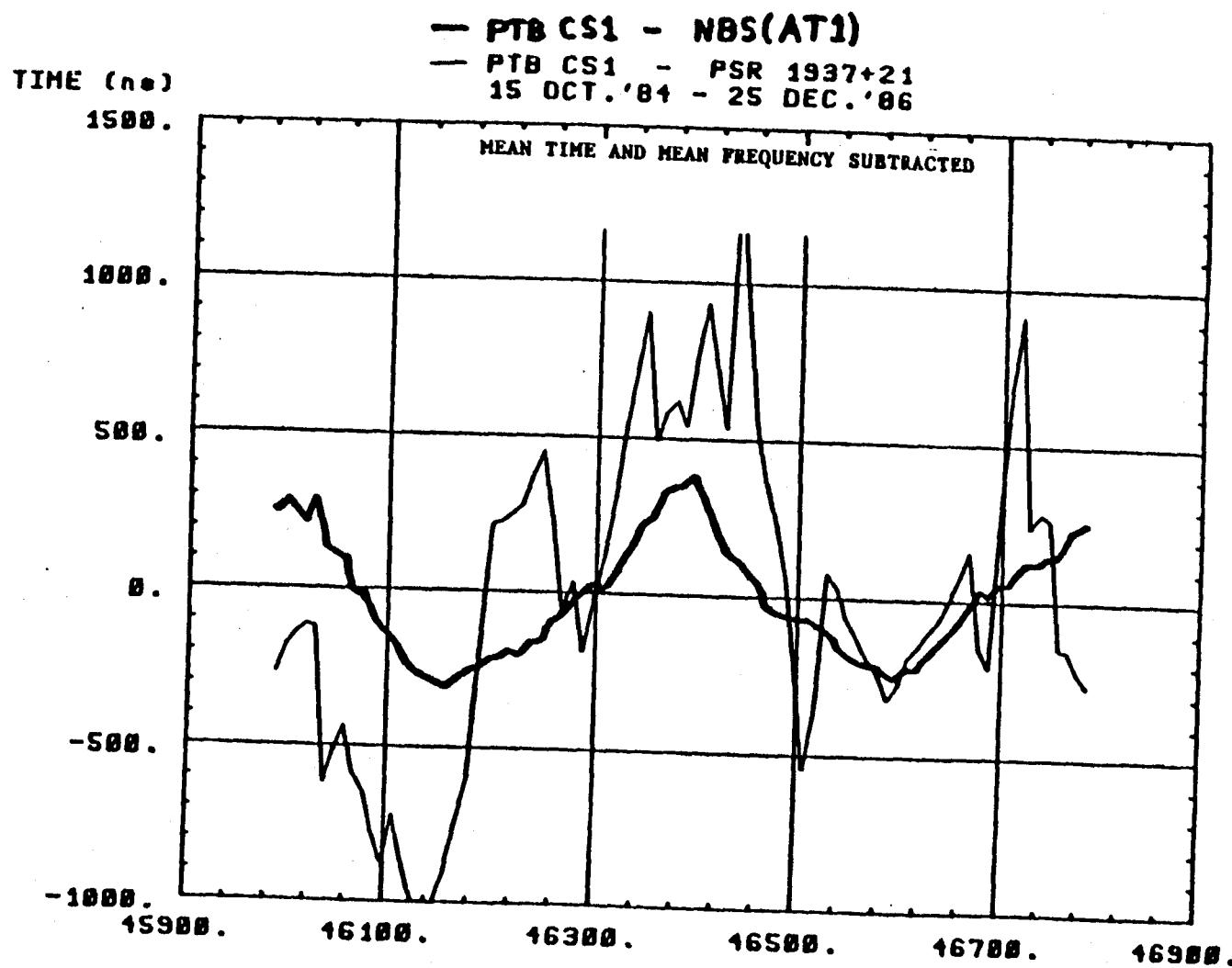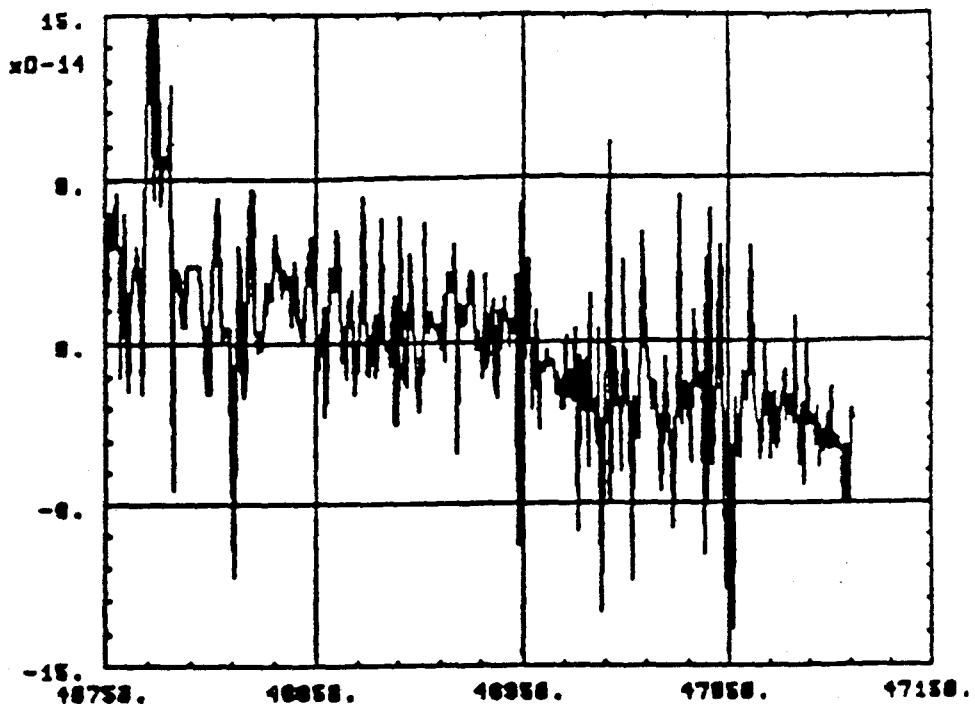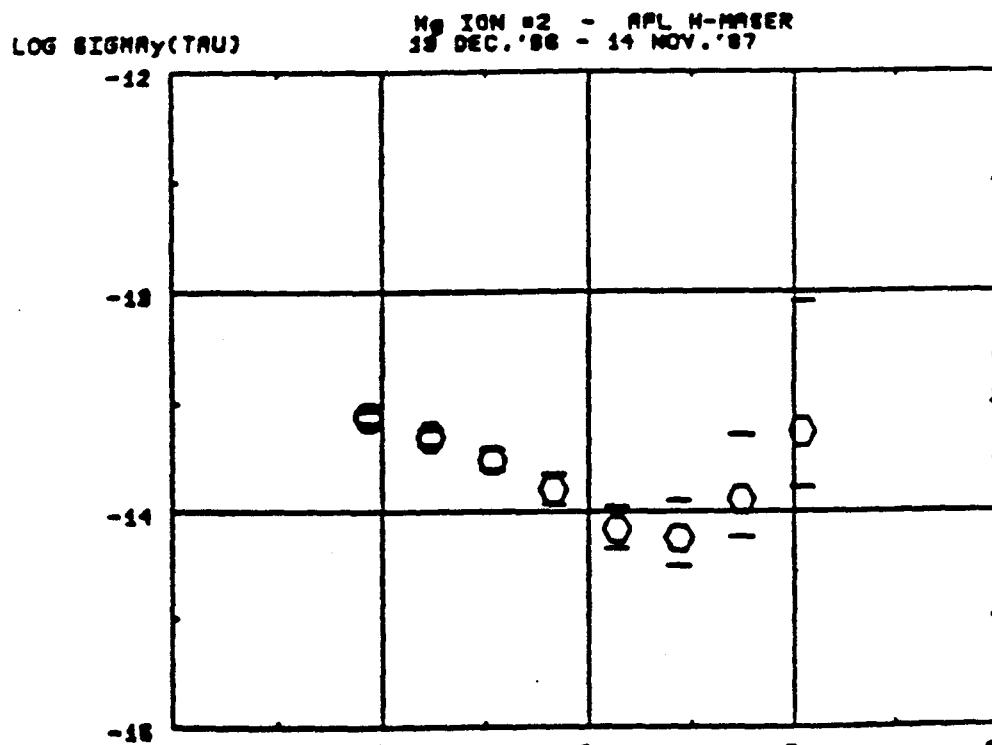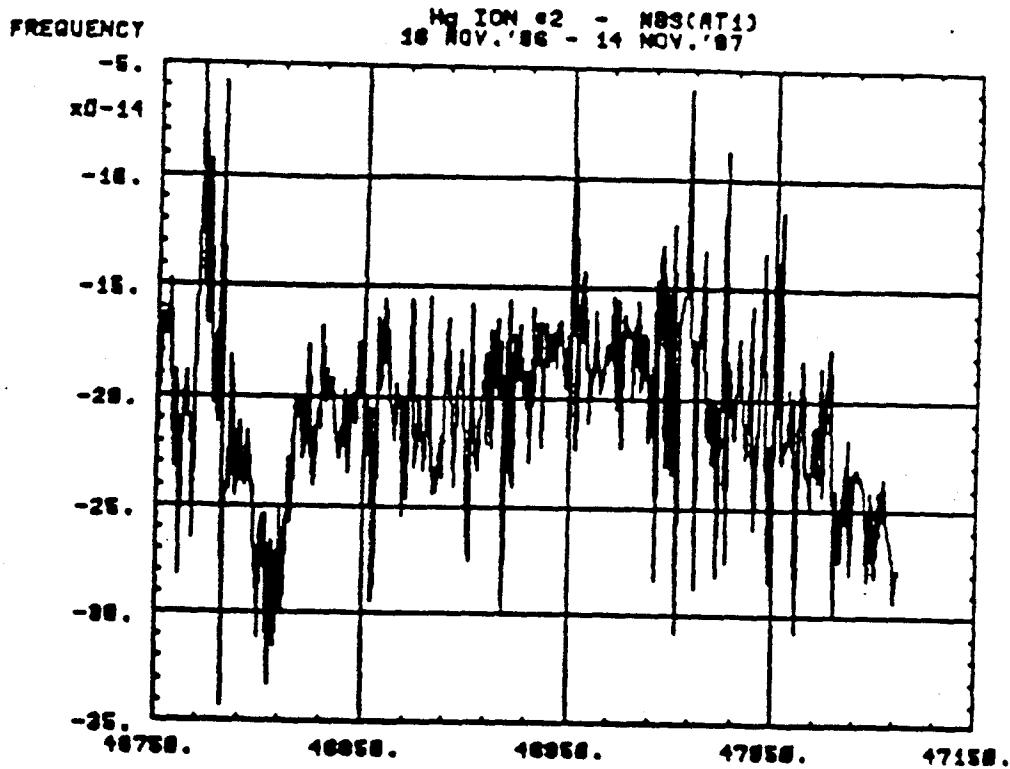
Figure 17b
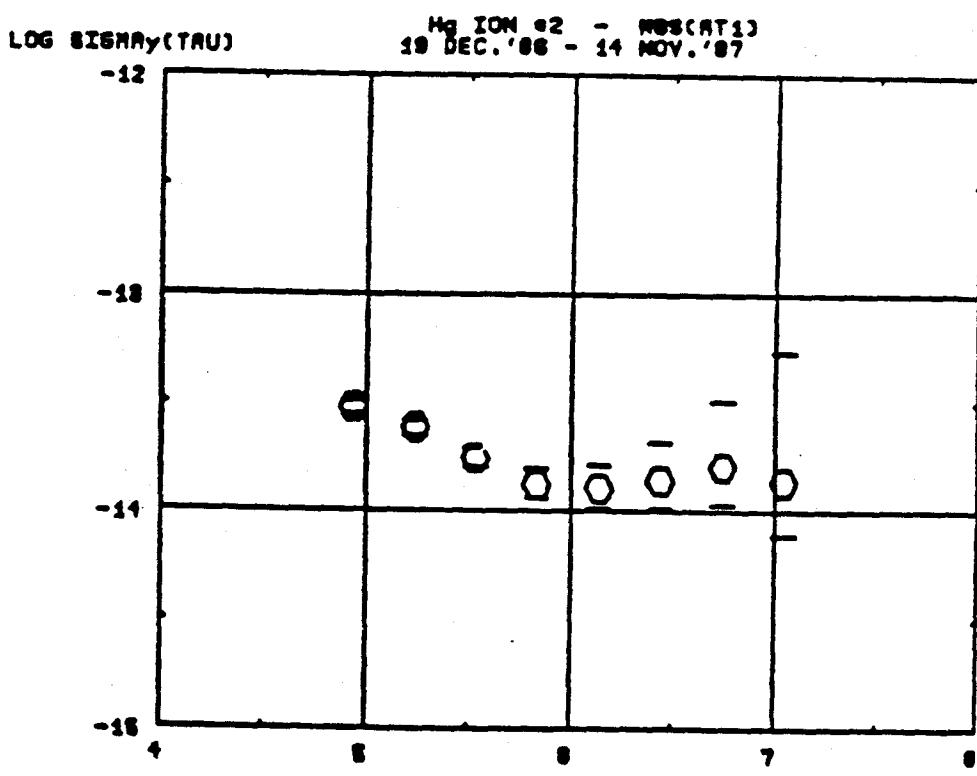
LOG TAU (Seconds)

Figure 18a

Figure 18b
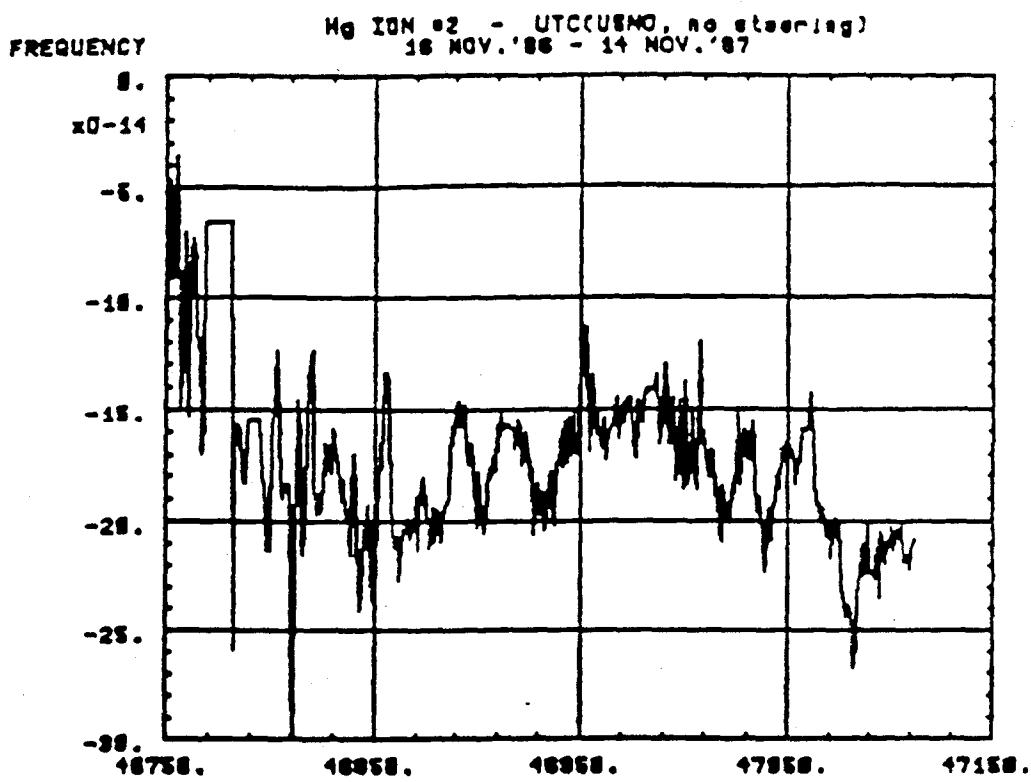
Figure 19a
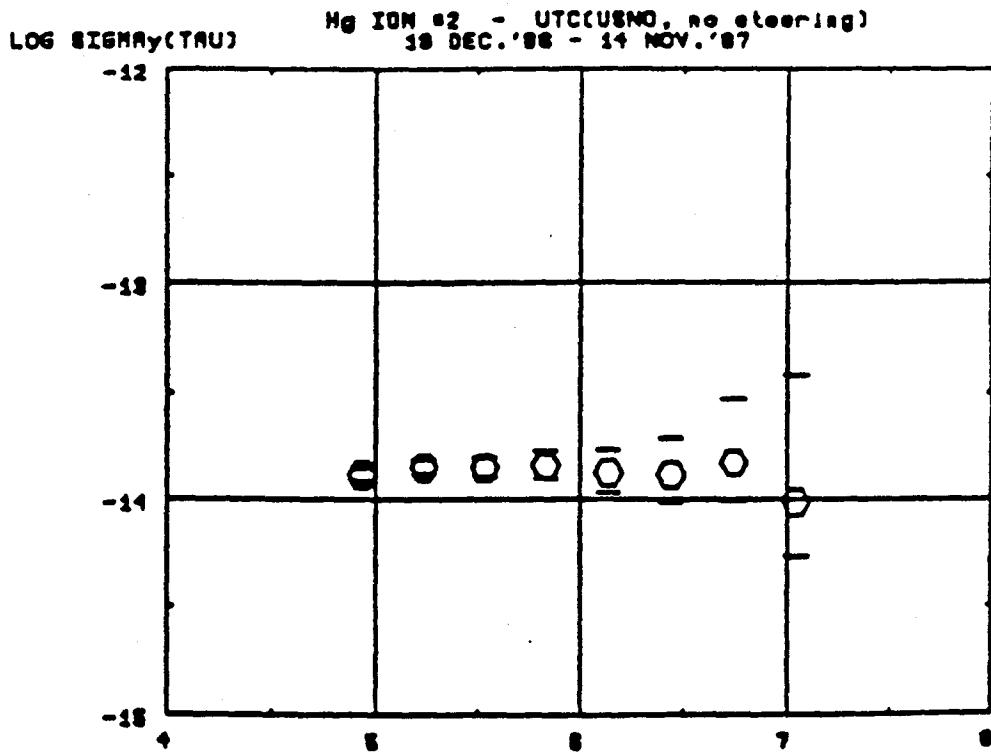
Figure 19b

19 DEC 86 — 15 NOV 87

Figure 20
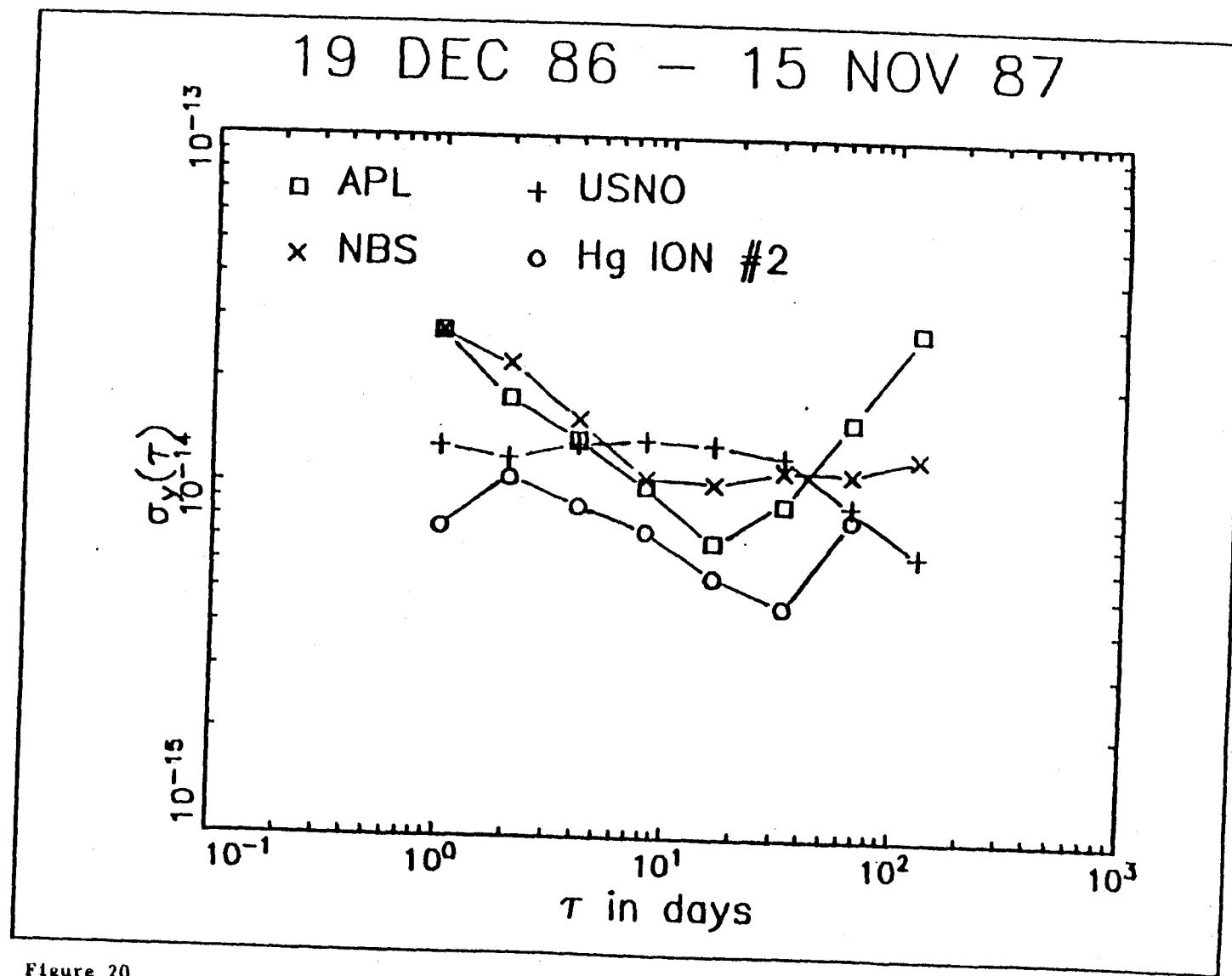
Figure 21a
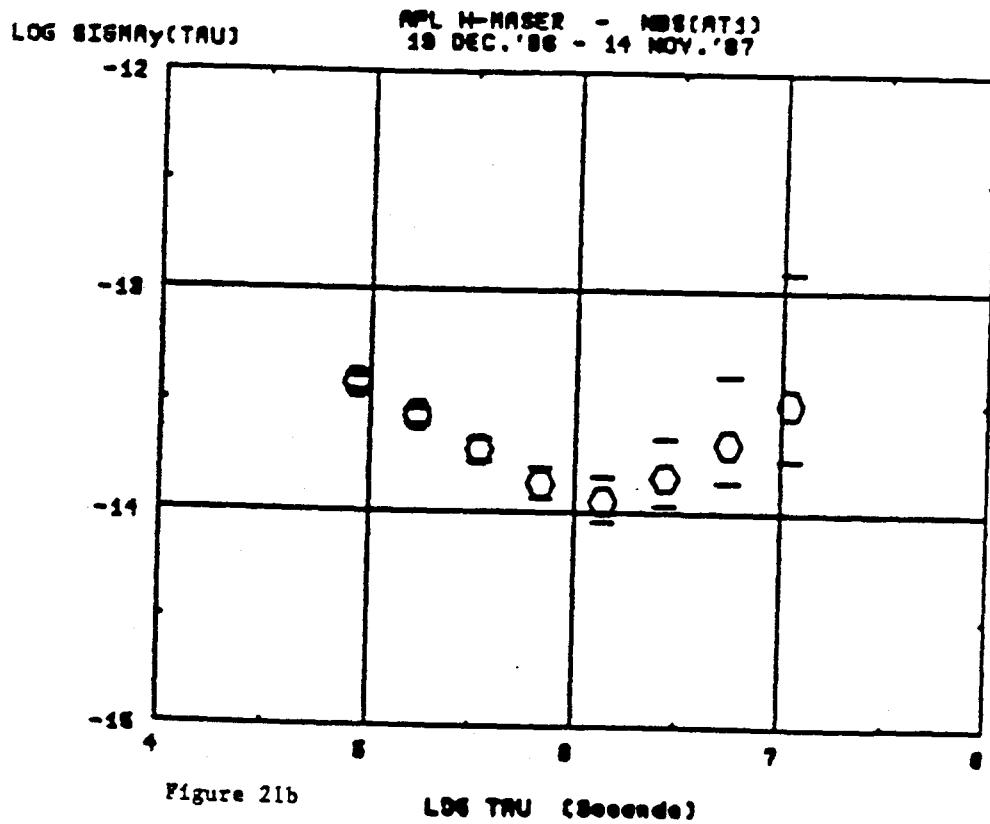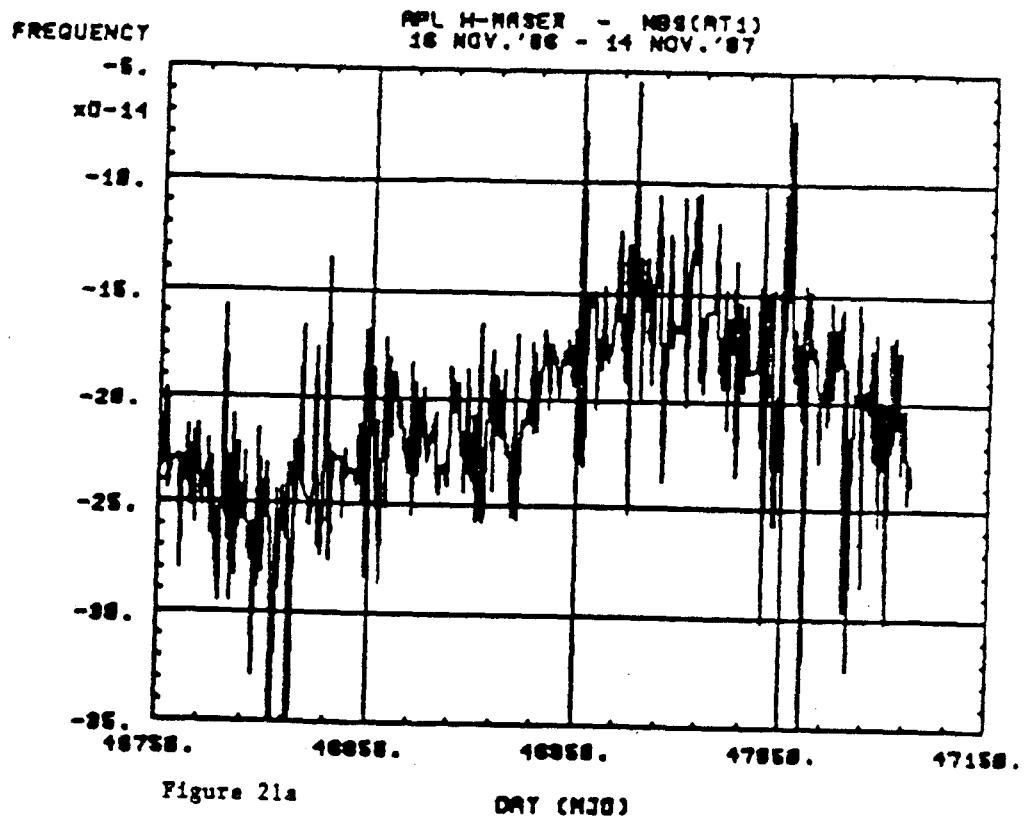
Figure 21b

LOG TAU (Seconds)

Figure 22a
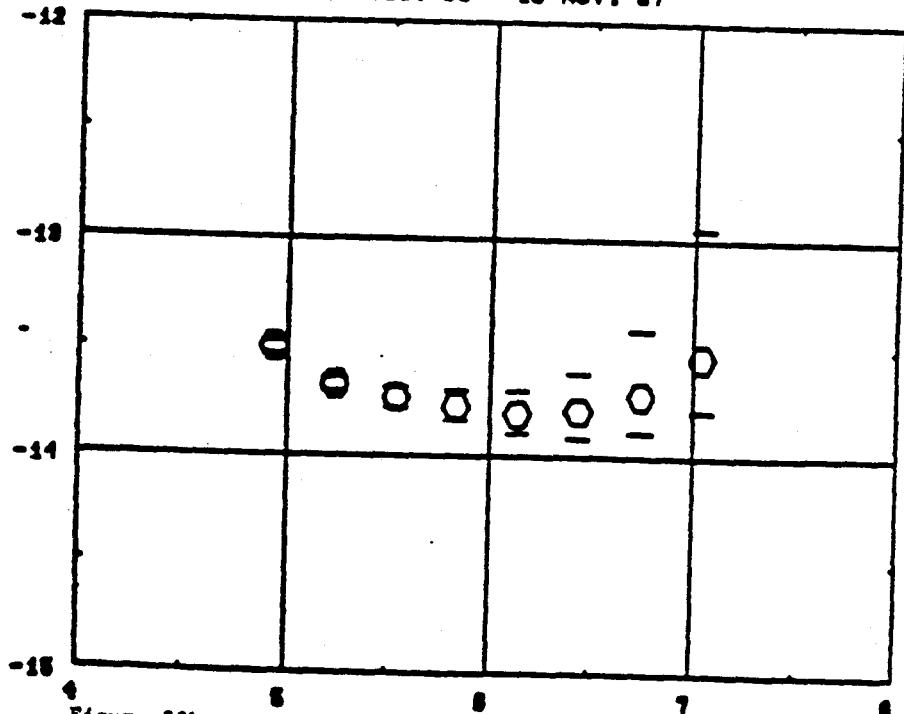
Figure 22b

Figure 23a

Figure 23b

Figure 24a
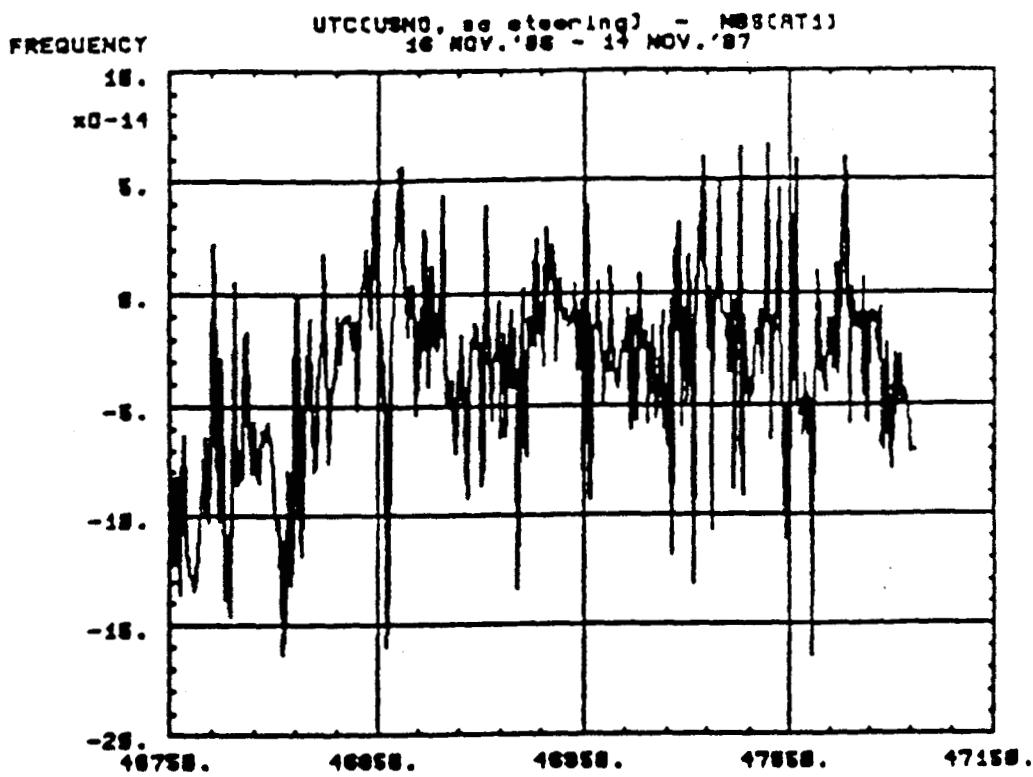
Figure 24b

CORR. COEF. (Hg ION #2 - UTC(USNO, NS)) VERSUS (Hg ION #2 - NBS(AT1))
15 NOV.'86 - 14 NOV.'87
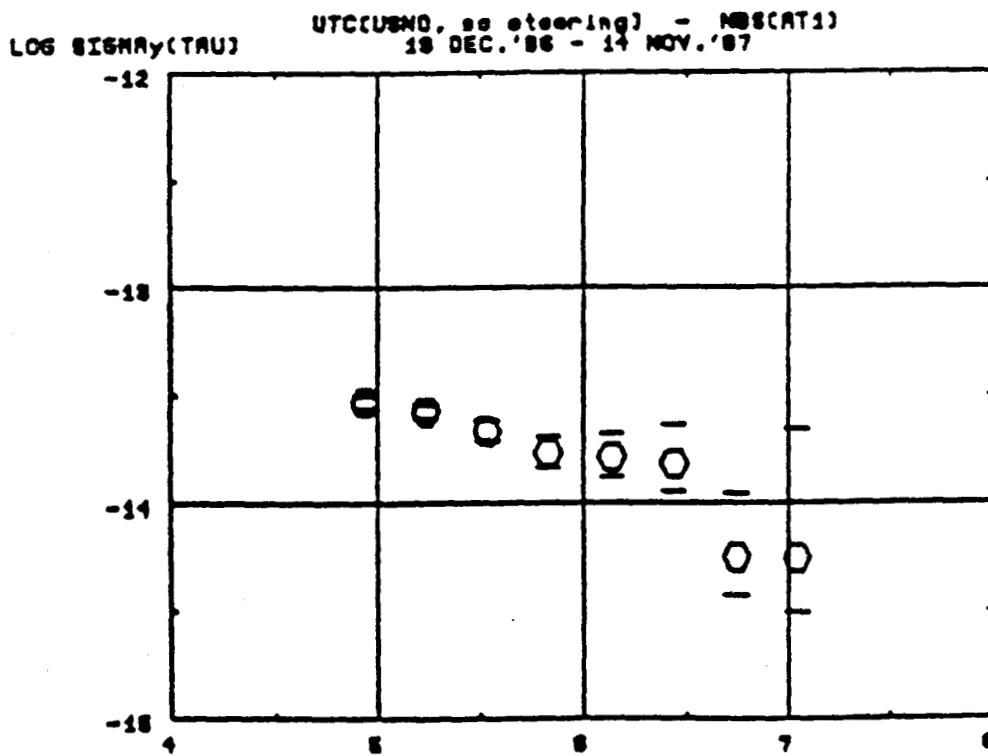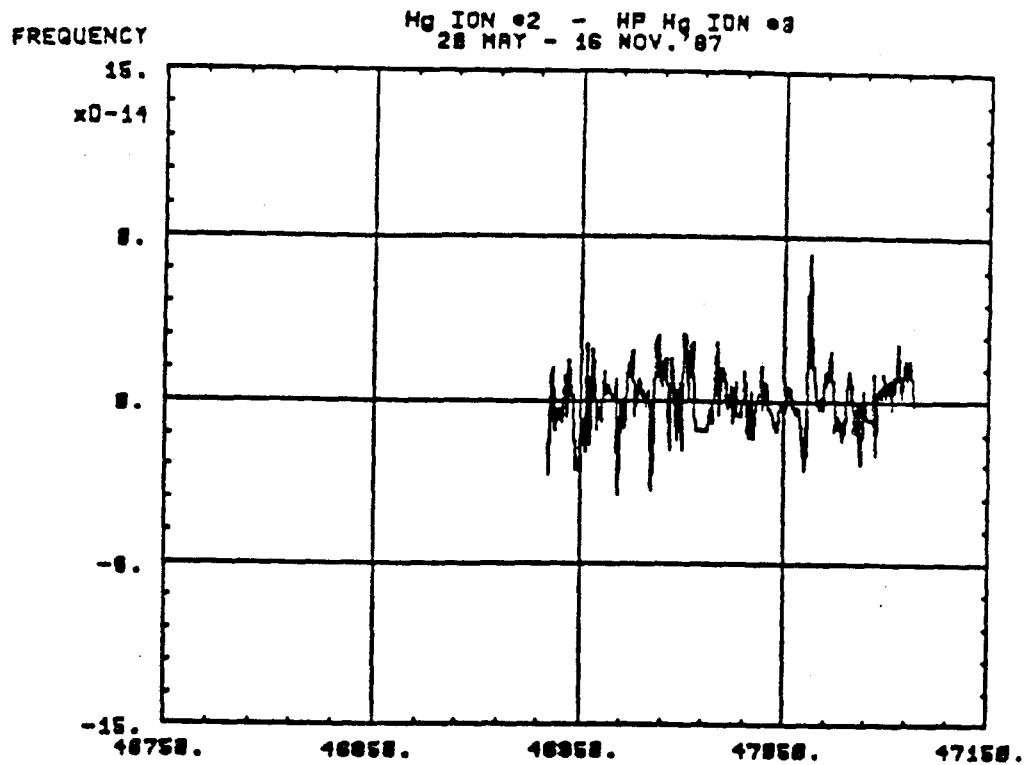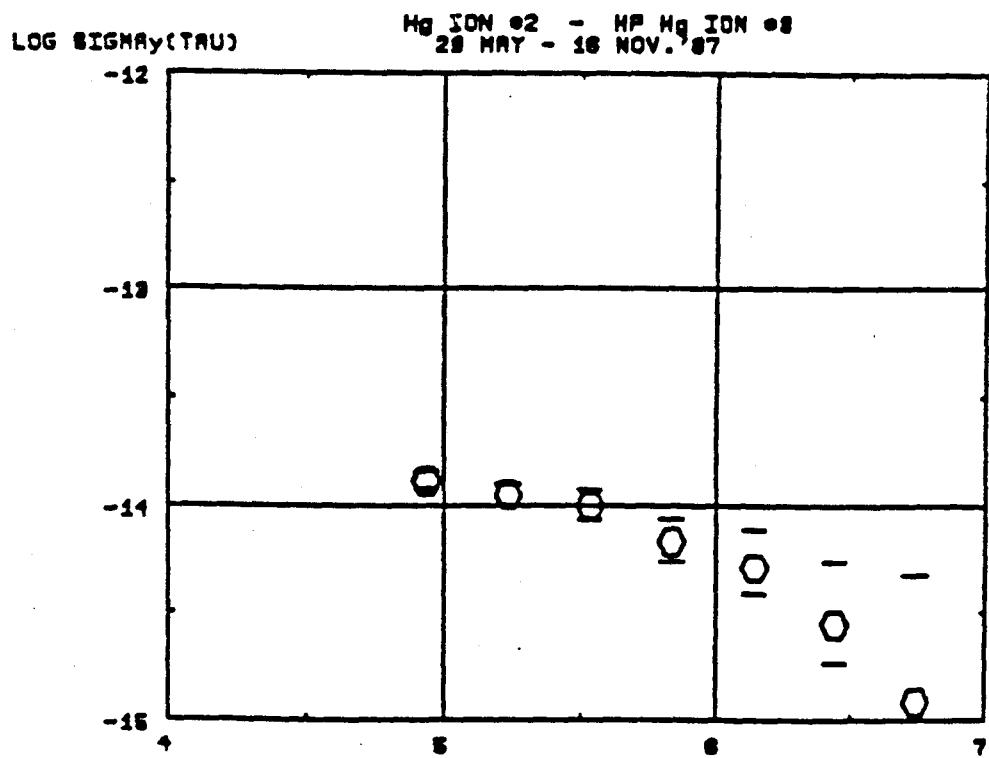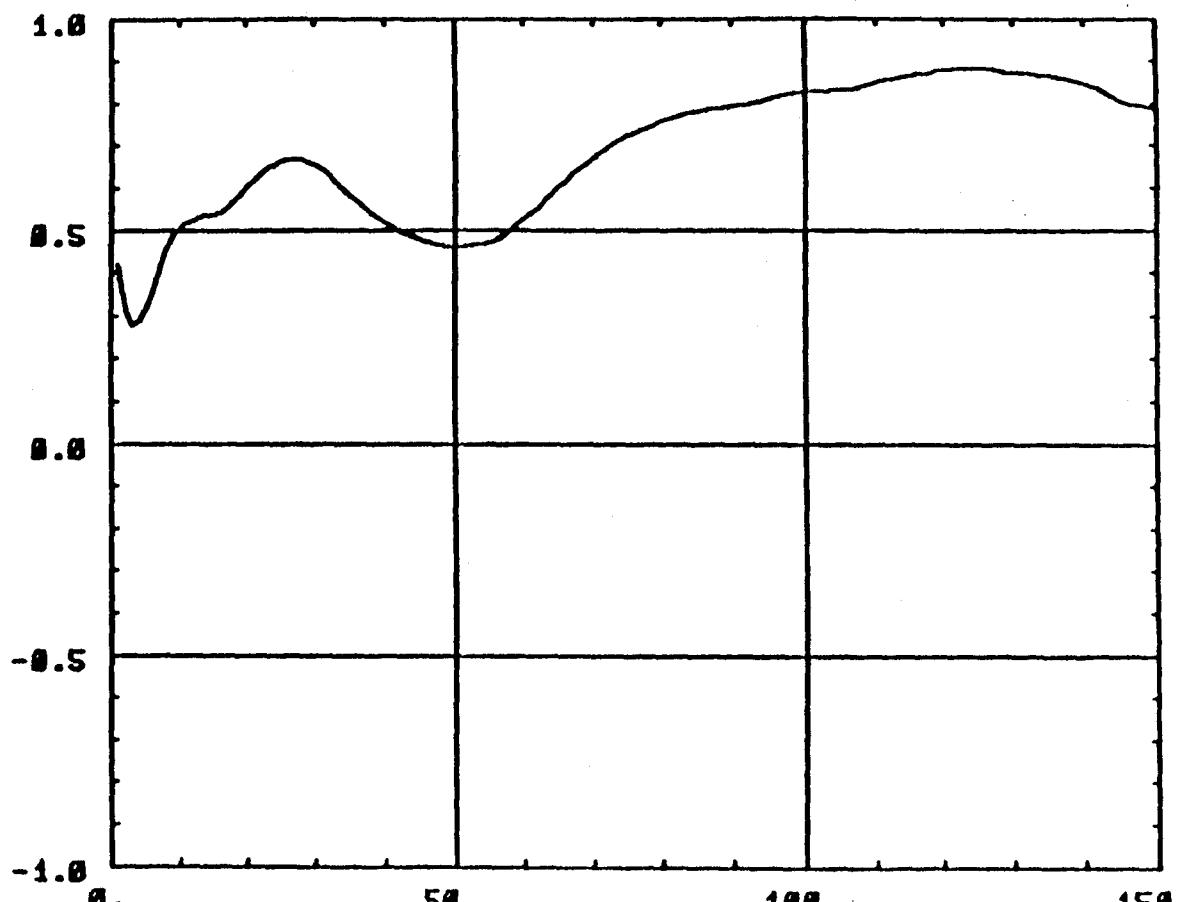
Figure 25   SAMPLE TIME, TAU (days)

380-27

CORR. COEF.   **(Hg ION #2 - APL H-MASER) vs. (Hg ION #3 - NBS(AT1))**
20 MAY - 5 NOV.'87
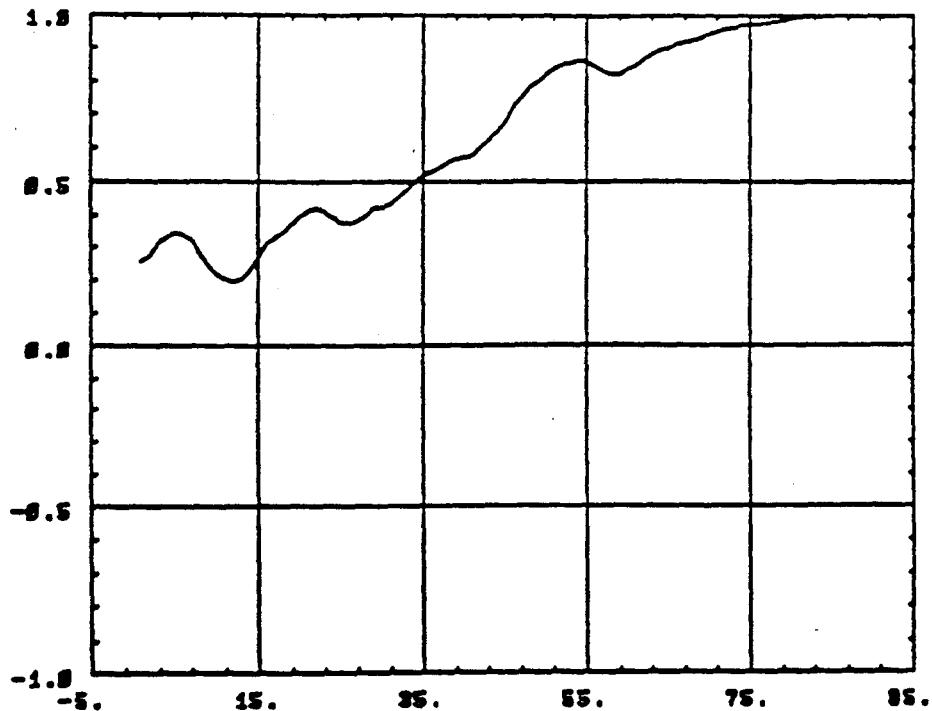
Figure 26a   **SAMPLE TIME, TAU (days)**

CORR. COEF.   **(Hg ION #3 - APL H-MASER) vs. (Hg ION #2 - NBS(AT1))**
20 MAY - 5 NOV.'87
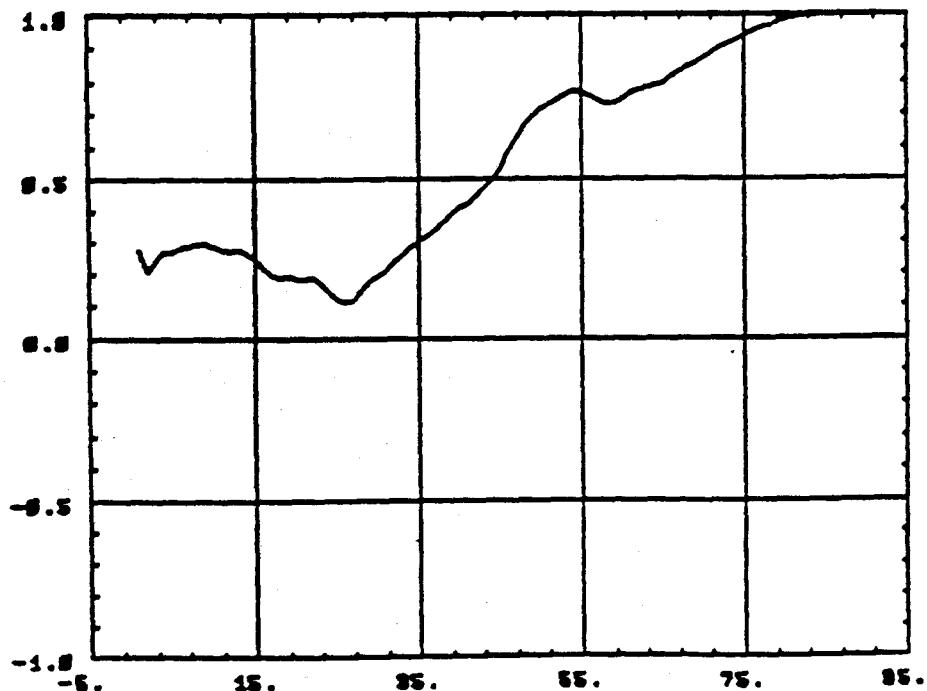
Figure 26b   **SAMPLE TIME, TAU (days)**
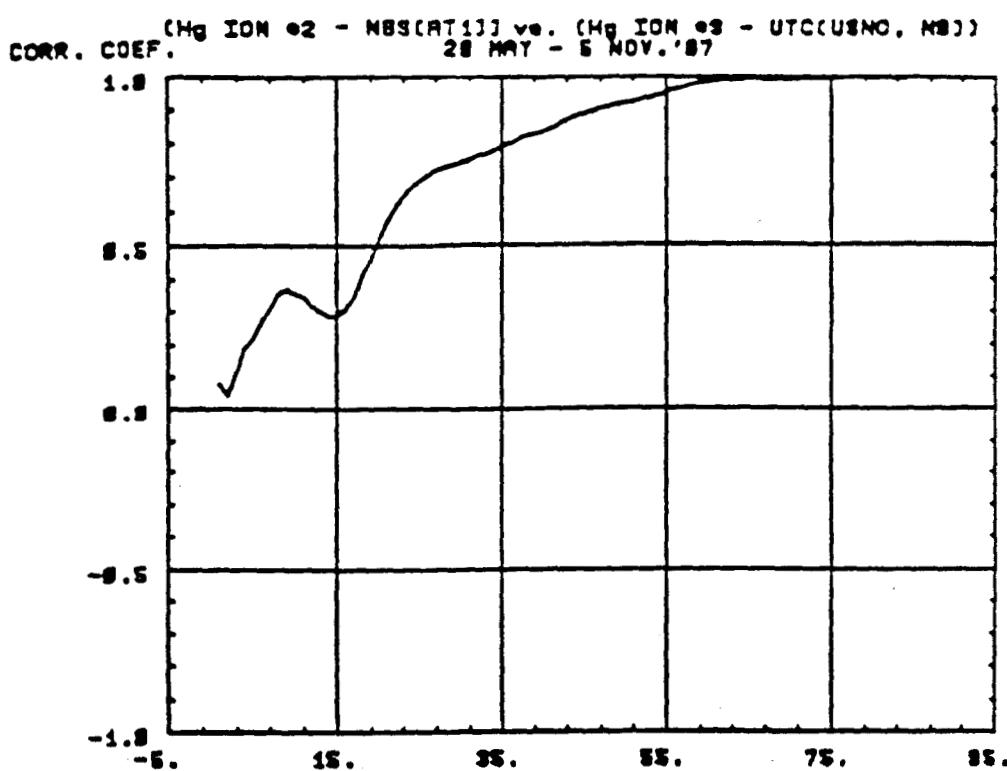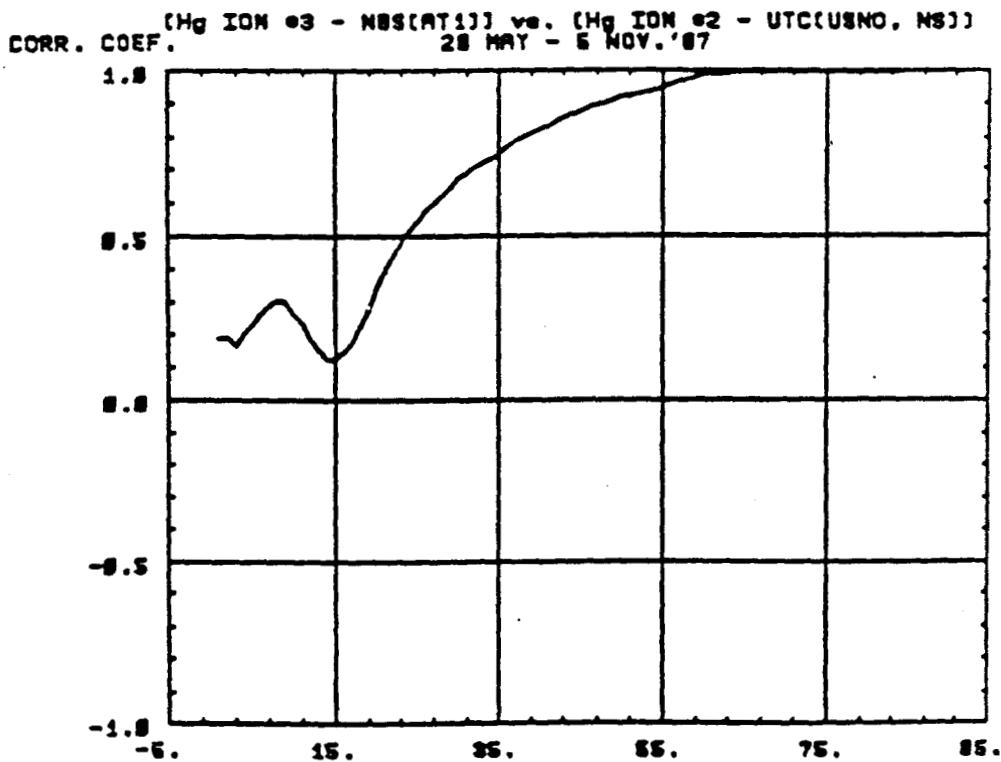
Figure 27a

Figure 27b

(Hg ION #2 - APL H-MASER) vs. (Hg ION #3 - UTC(USNO, MS))
28 MAY -5 NOV.'87
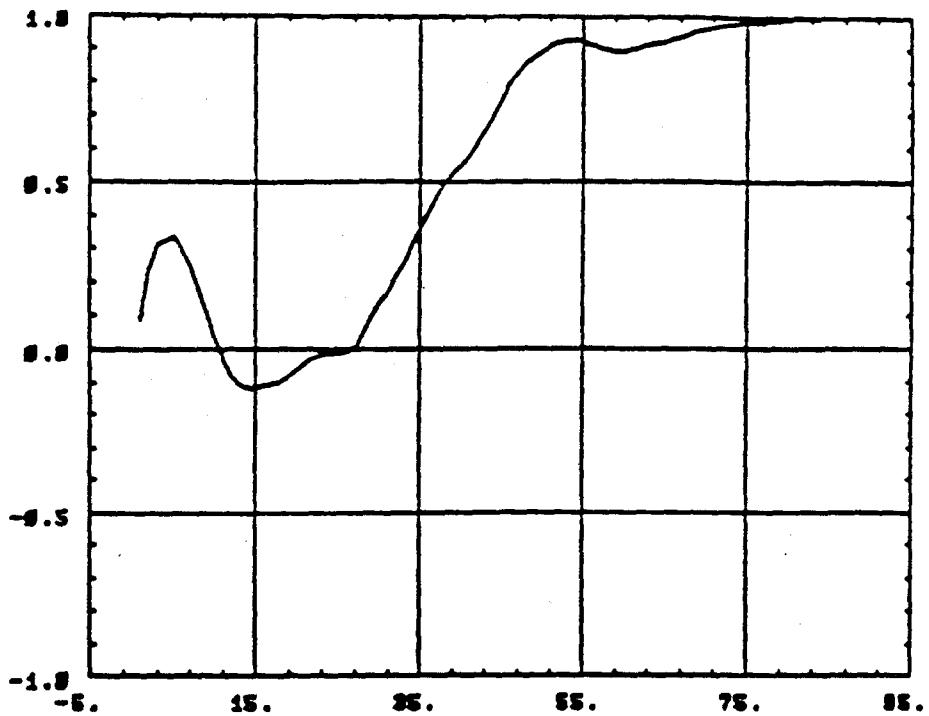
CORR. COEF.

Figure 28a   SAMPLE TIME TAU   (days)

(Hg ION #3 - APL H-MASER) vs. (Hg ION #2 - UTC(USNO, MS))
28 MAY - 5 NOV.'87
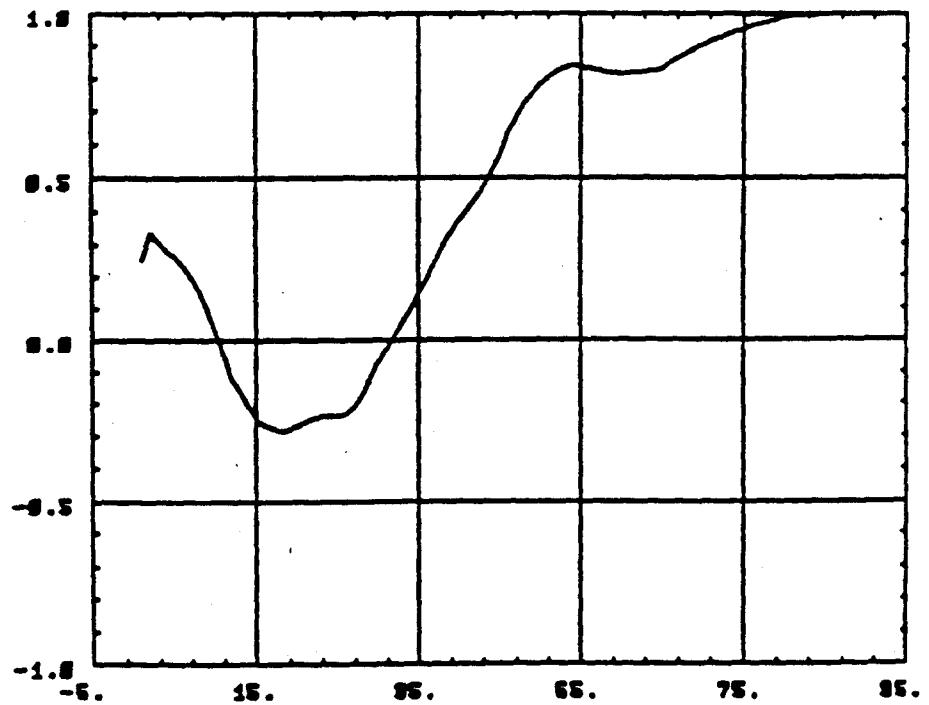
CORR. COEF.

Figure 28b   SAMPLE TIME, TAU   (days)

(Hg ION #2 - CRPL H-MRSER vs. (NBS(AT1) - UTC(USNO, NS))
CORR. COEF.   28 MAY - 5 NOV.'87
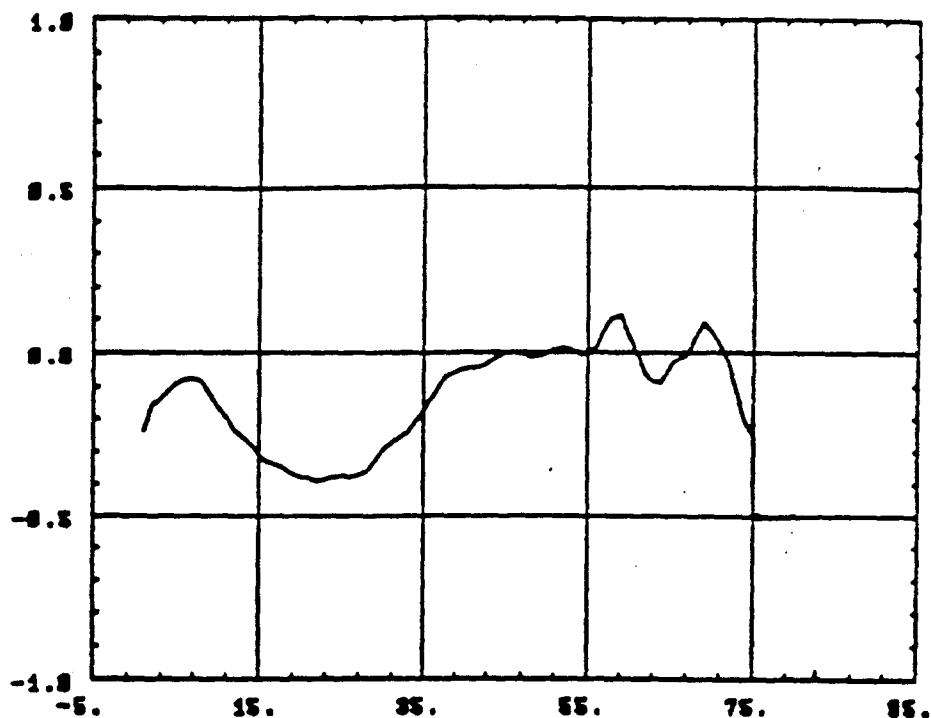
Figure 29a   SAMPLE TIME, TAU   (days)

(Hg ION #2 - NBS(AT1)) vs. (CRPL H-MRSER - UTC(USNO, NS))
CORR. COEF.   28 MAY - 5 NOV.'87
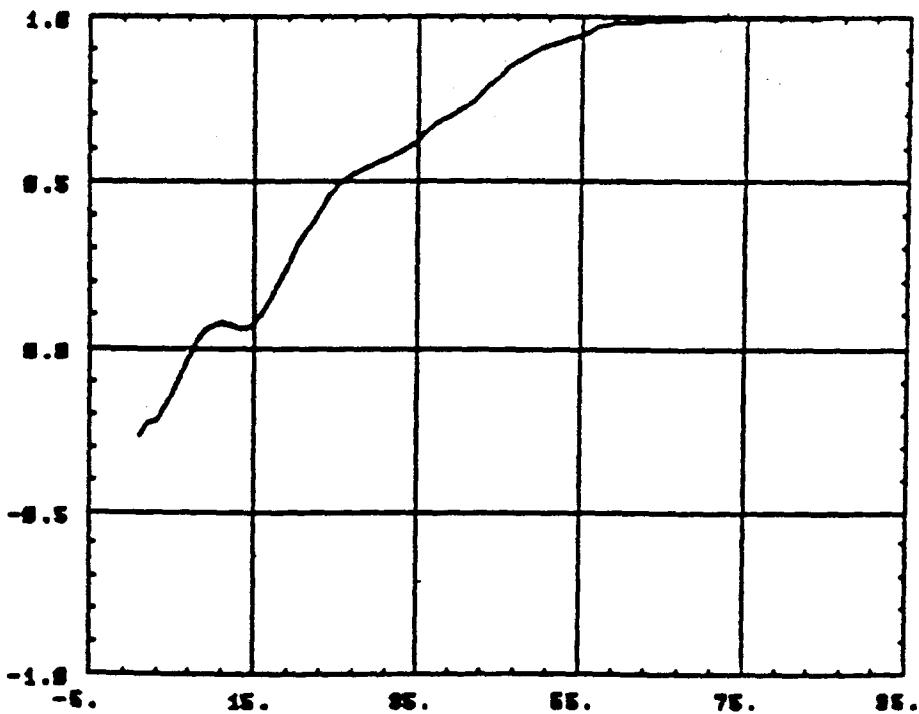
Figure 29b   SAMPLE TIME, TAU   (days)

380-31

FREQUENCY DRIFT ESTIMATES (in units of 10^{-15}/DAY)

USING 2nd DIFFERENCE ESTIMATOR FOR MJD 46935 - 47104

HG ION #2	HG ION #3	APL H-MASER	REF. STD.
-0.51	-0.52	-0.31	- NBS(AT1)
-0.44	-0.45	-0.25	- UTC(USNO, NS)
-0.38	-0.38	-0.19	- UTC(PTB)
-0.44 +/-0.06	-0.45 +/-0.07	-0.25 +/- 0.06	AVERAGE

Figure 30